Article

Ex utero mouse embryogenesis from pre-gastrulation to late organogenesis

https://doi.org/10.1038/s41586-021-03416-3

Received: 30 June 2020

Accepted: 4 March 2021

Published online: 17 March 2021

Check for updates

Alejandro Aguilera-Castrejon[1,10,11]✉, Bernardo Oldak[1,10], Tom Shani[1], Nadir Ghanem[2], Chen Itzkovich[3], Sharon Slomovich[4], Shadi Tarazi[1], Jonathan Bayerl[1], Valeriya Chugaeva[1], Muneef Ayyash[1], Shahd Ashouokhi[1], Daoud Sheban[1], Nir Livnat[1], Lior Lasman[1], Sergey Viukov[1], Mirie Zerbib[1], Yoseph Addadi[5], Yoach Rais[6], Saifeng Cheng[6], Yonatan Stelzer[6], Hadas Keren-Shaul[7], Raanan Shlomo[8], Rada Massarwa[1,11,12], Noa Novershtern[1,11], Itay Maza[4,9,11]✉ & Jacob H. Hanna[1,11]✉

The mammalian body plan is established shortly after the embryo implants into the maternal uterus, and our understanding of post-implantation developmental processes remains limited. Although pre- and peri-implantation mouse embryos are routinely cultured in vitro[1,2], approaches for the robust culture of post-implantation embryos from egg cylinder stages until advanced organogenesis remain to be established. Here we present highly effective platforms for the ex utero culture of post-implantation mouse embryos, which enable the appropriate development of embryos from before gastrulation (embryonic day (E) 5.5) until the hindlimb formation stage (E11). Late gastrulating embryos (E7.5) are grown in three-dimensional rotating bottles, whereas extended culture from pre-gastrulation stages (E5.5 or E6.5) requires a combination of static and rotating bottle culture platforms. Histological, molecular and single-cell RNA sequencing analyses confirm that the ex utero cultured embryos recapitulate in utero development precisely. This culture system is amenable to the introduction of a variety of embryonic perturbations and micro-manipulations, the results of which can be followed ex utero for up to six days. The establishment of a system for robustly growing normal mouse embryos ex utero from pre-gastrulation to advanced organogenesis represents a valuable tool for investigating embryogenesis, as it eliminates the uterine barrier and allows researchers to mechanistically interrogate post-implantation morphogenesis and artificial embryogenesis in mammals.

Understanding the developmental processes that lead to the formation of tissues and organs represents a fundamental question in developmental biology. In mammals, this process takes place after the embryo implants into the uterus, which makes it relatively inaccessible for observation and manipulation[3,4]. Consequently, the sequence of developmental events that takes place from pre-gastrulation to organogenesis remains to be fully understood and is difficult to manipulate. Establishing culture conditions that sustain the proper long-term development of post-implanted mouse embryos outside the uterine environment remains a challenge. Several useful culture techniques have been proposed since the 1930s, including culturing the embryos in conventional static conditions[5,6], in rotating bottles on a drum ('roller culture systems')[7] or in circulator systems[8]. However, these platforms remain highly inefficient for normal embryo survival, use already gastrulating embryos and are limited to short periods of time[9,10], as the embryos begin to display developmental anomalies as early as 24 h after culture initiation. Thus, stable and efficient protocols for extended culturing of pre-gastrulating mouse embryos until advanced organogenesis are still required[11].

Enhanced ex utero roller culture platform

We set out to test whether some of the newly established cell culture supplements or biomechanical principles that have arisen in stem cell research could be helpful for addressing this challenge (for example, pressure control, supplements or synthetic sera[12–14]). We used the roller culture system on a drum and integrated it with a customized, in-house-developed electronic gas regulation module that not only allows the precise and sensitive control of O_2 and CO_2 levels, but also allows atmospheric gas pressure to be controlled (Fig. 1a, b, Extended Data Fig. 1, Supplementary Video 1). The latter was motivated by the ability of pressure to enhance oxygen delivery

[1]Department of Molecular Genetics, Weizmann Institute of Science, Rehovot, Israel. [2]Department of Obstetrics and Gynecology, Rambam Health Care Campus, Haifa, Israel. [3]The Clinical Research Institute at Ramban (CRIR), Rambam Health Care Campus, Haifa, Israel. [4]Bruce Rappaport Faculty of Medicine, Israel Institute of Technology - Technion, Haifa, Israel. [5]Department of Life Sciences Core Facilities, Weizmann Institute of Science, Rehovot, Israel. [6]Department of Molecular Cell Biology, Weizmann Institute of Science, Rehovot, Israel. [7]Department of Life Sciences Core Facilities, Weizmann Institute of Science, Rehovot, Israel. [8]Arad Technologies Ltd, Ashdod, Israel. [9]Gastroenterology Unit, Rambam Health Care Campus, Haifa, Israel. [10]These authors contributed equally: Alejandro Aguilera-Castrejon, Bernardo Oldak. [11]These authors jointly supervised this work: Alejandro Aguilera-Castrejon, Rada Massarwa, Noa Novershtern, Itay Maza, Jacob H. Hanna. [12]Deceased: Rada Massarwa. ✉e-mail: alejandroac@weizmann.ac.il; i_maza@rambam.health.gov.il; jacob.hanna@weizmann.ac.il

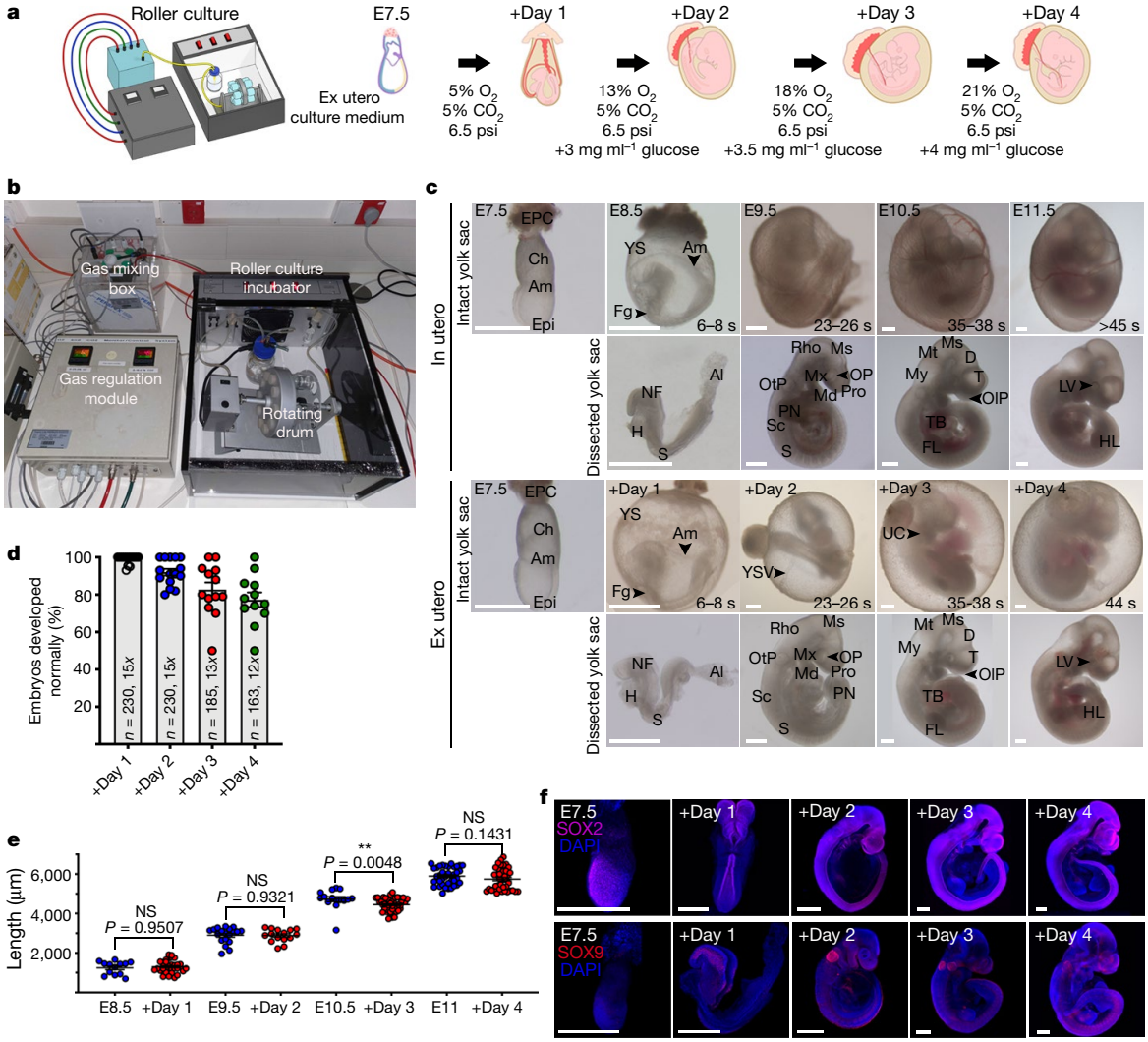

Fig. 1 | Ex utero culture system for growing mouse late-gastrulating embryos until advanced organogenesis. a, Schematic of the E7.5 embryo ex utero culture platform. **b**, Electronic gas and pressure regulation module connected to the roller culture incubator system. **c**, Bright-field images of embryos developing in utero from E7.5 to E11.5 and equivalent embryos cultured ex utero. **d**, Percentage of developmentally normal embryos per culture day. *n*, total number of embryos; *x*, number of experiments. All data are mean ± s.e.m. **e**, Quantification of embryonic length for in utero and cultured embryos. Dots represent individual embryos. Numbers of embryos, left to right: in utero, 13, 19, 15, 38; ex utero, 32, 15, 43, 41; NS, not significant; Mann–Whitney test. **f**, SOX2 and SOX9 whole-mount immunofluorescence of embryos developed ex utero from E7.5. Images represent a minimum of three biological replicates. Am, amnion; Al, allantois; Ch, chorion; D, diencephalon; Epi, epiblast; EPC, ectoplacental cone; Fg, foregut pocket; FL, forelimb bud; H, heart; HL, hindlimb bud; LV, lens vesicle; Md, mandibular arch; Ms, mesencephalon; Mt, metencephalon; Mx, maxillary arch; My, myelencephalon; NF, neural folds; OlP, olfactory placode; OP, optic pit; OtP, otic pit; PN, posterior neuropore; Pro, prosencephalon; Rho, rhombencephalon; S, somites; Sc, spinal cord; T, telencephalon; TB, tail bud; UC, umbilical cord; YS, yolk sac; YSV, yolk sac vessel. Scale bars, 500 μm.

to tissues and by demonstrations that atmospheric pressure can alter cell growth[13,14]. We established conditions that support the growth of E7.5 late-gastrulating embryos (neural plate and headfold stage[15]) until the hindlimb formation stage (around E11) with high efficiency (Fig. 1a–c, Supplementary Video 2, Extended Data Fig. 2a, b). First, a mixture of 25% Dulbecco's modified Eagle's medium (DMEM), 50% rat serum and 25% human umbilical cord blood serum (HCS) consistently supports embryo growth with much higher efficiency than rat serum only (Extended Data Fig. 2b), and we designated this medium as ex utero culture medium (EUCM). Notably, supplementing EUCM with extra glucose every 24 h and until the end of the culture period was essential for overcoming developmental abnormalities after two days in culture (Extended Data Fig. 2b). The application of sequential increases in O_2 levels every 24 h, from 5% O_2 at E7.5, 13% at E8.5, 18% at E9.5, to 21% O_2 at E10.5 was most optimal (Extended Data Fig. 2b). In addition, normal and efficient development depended on the maintenance of a gas pressure of 6–7 psi (Extended Data Fig. 2b). This protocol yielded approximately 77% normal embryo development after four days in culture in different mouse strains (Fig. 1d, Extended Data Fig. 2c). After four days, the embryos started to show abnormalities, yolk sac circulation abruption and pericardial effusion, and quickly died overnight. The latter effects are consistent with the development of hydrops fetalis due to insufficient oxygenation and nutrient supply by the ex utero system (given the lack of maternal blood supply in this setting) that no longer matches the increased body size at E11.

We evaluated previously defined morphological landmarks[16] to assess appropriate embryo development ex utero (Fig. 1c, Supplementary Video 3, Supplementary Methods). On the last day of culture, maximum embryo growth was reached at about 44 somites, equivalent to approximately E11 (Theiler stage 18). The length of the cultured embryos was comparable to matched in utero embryos (Fig. 1e). We analysed eleven developmental markers, all of which showed consistent

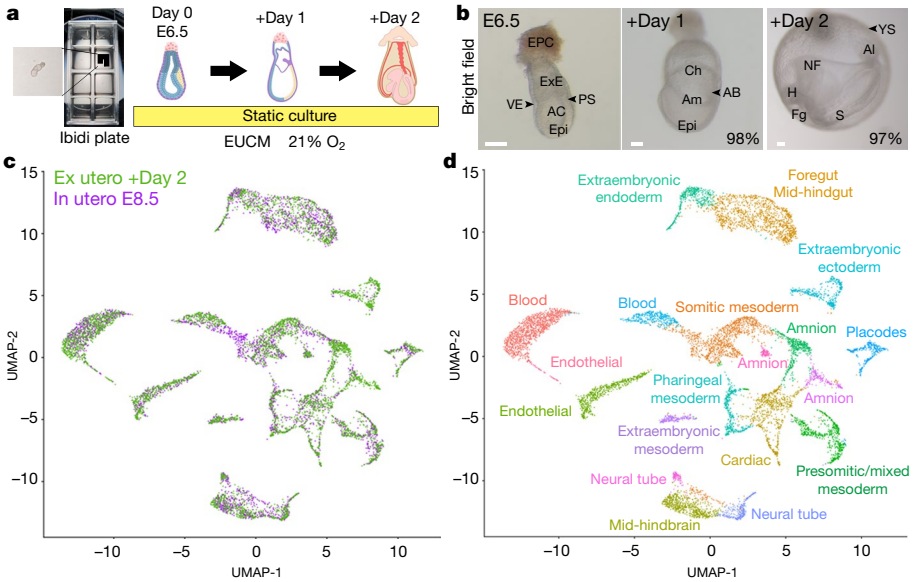

Fig. 2 | Defining conditions for recapitulating mouse gastrulation ex utero. **a**, Static culture protocol for growing gastrulating embryos until somitogenesis. **b**, Bright-field images of embryos developing ex utero from E6.5 until E8.5; bottom right, percentage of properly developed embryos. $n = 421$ at +Day 1, $n = 399$ at +Day 2. **c**, scRNA-seq analysis of in utero E8.5 embryos (purple dots) versus E6.5 +Day 2 ex utero developing embryos (green dots). UMAP plot displaying individual cells ($n = 6,358$ ex utero +Day 2; $n = 4,349$ in utero E8.5). **d**, Cell lineage annotation of clusters based on marker genes of the major cell types identified in E8.5 mouse embryos[19]. Points are coloured according to their assigned cell cluster. AB, allantoic bud; ExE, extraembryonic ectoderm; PS, primitive streak; VE, visceral endoderm. Scale bars, 100 µm.

spatio-temporal gene expression patterns between embryos that developed in utero or ex utero (Fig. 1f, Extended Data Figs. 3, 4, Supplementary Video 4). Mouse transgenic lines expressing the GFP reporter for imprinting erasure of the *Dlk1–Dio3* intergenic differentially methylated region (DMR)[17] in migrating primordial germ cells, or under tissue-specific promoters (*Wnt1-Cre* and *Isl1-Cre*), showed that the GFP expression patterns in the cultured transgenic embryos resemble those of in utero embryos (Extended Data Fig. 5). These data suggest that the ex utero cultured embryos recapitulate development properly until approximately the 44-somite stage.

Capturing authentic gastrulation ex utero

We aimed to expand the ex utero culture protocol by establishing conditions to grow the mouse embryo from pre-gastrulation stages (E5.5–6.5). Explanted E6.5 embryos grown in rotating bottles either in 5% or 21% O_2, or under previously described static conditions[18], did not develop beyond the early somite stage (Extended Data Fig. 6d, e, o, Supplementary Discussion). Thus, we set out to devise alternative culture parameters for growing embryos from E6.5 to E8.5 in static conditions (Fig. 2a, Extended Data Fig. 6). The following conditions were optimized: 25% DMEM, 50% rat serum and 25% HCS in 21% O_2. The latter supported the development of early-streak embryos (E6.5) in static culture until the early somite stage (48 h) with up to 97% efficiency (Fig. 2a, b, Extended Data Fig. 6a, b). Embryos grown in utero or ex utero were equivalent morphologically and in the expression of all lineage markers analysed (Extended Data Fig. 7). The robustness of these culture conditions allowed in toto imaging of the gastrulating mouse embryo for 58 h (Supplementary Video 5).

To characterize the various lineages present in the embryos, and to identify to what extent the global transcriptional profile of embryos developing in culture mimics their in utero counterparts, we performed single-cell RNA sequencing (scRNA-seq) on embryos grown ex utero at day two (E6.5 + 2 days) and compared the results to those from cells obtained from equivalent embryos developing in utero (Extended Data Fig. 8a, b). Clustering analysis based on differentially expressed genes revealed 19 different cell states (Extended Data Fig. 8c). The distribution of cell states overlapped strongly between in utero and ex utero embryos (Fig. 2c). The identity of each cluster was annotated using specific marker genes of cell lineages that have been previously defined by single-cell transcriptomics of early mouse embryos[19,20] (Extended Data Fig. 8c, e). We identified derivatives of the three germ layers as well as extraembryonic tissues, and the profile of cell types found in embryos developing ex utero was equivalent to that in utero (Fig. 2c, d). In summary, the alternative static conditions generated herein faithfully recapitulate embryo development ex utero from the onset of gastrulation until somitogenesis (E6.5 to E8.5).

Extended ex utero embryogenesis

We next tested the ability to bridge mouse pre-gastrulation development to advanced organogenesis in culture by combining our static and roller culture protocols. After two days of static culture from E6.5, early somite-stage embryos (E8.5) were transferred into the roller culture protocol, which allowed normal development of embryos isolated at early-streak stages until the hindlimb formation stage (E11), with 40% efficiency (Fig. 3a–c, Extended Data Fig. 6b, Supplementary Video 6). Only those embryos cultured in normoxia from E6.5 to E8.5 were able to continue growing after being moved to the roller culture system, which indicates that these conditions support appropriate embryo development (Extended Data Fig. 6a, b, g, h). Culturing the embryos in a constant atmosphere of 21% oxygen through 5 days of culture increased the efficiency of development to 55% (Extended Data Fig. 9a–d). The same protocol and conditions were able to support the development of pre-primitive streak (E5.5) mouse embryos for a total of 6 days ex utero, with 46% of embryos reaching E8.5 and about 20% reaching the 42-somite stage (Fig. 3d, Extended Data Fig. 9e–h, Supplementary Video 7). Even though a delay of 1–2 pairs of somites seemed to arise in the timing of developmental events from E6.5, and of 2–4 pairs of somites from E5.5, embryo and tissue morphogenesis proceeded properly (Fig. 3b, d, Extended Data Fig. 9). As with in vivo development, the embryos increased in size from about 200 µm at E6.5 to about 5.4 mm at the 44-somite stage (Extended Data Fig. 9a–d). Immunofluorescence analyses of developmental genes confirmed that these markers

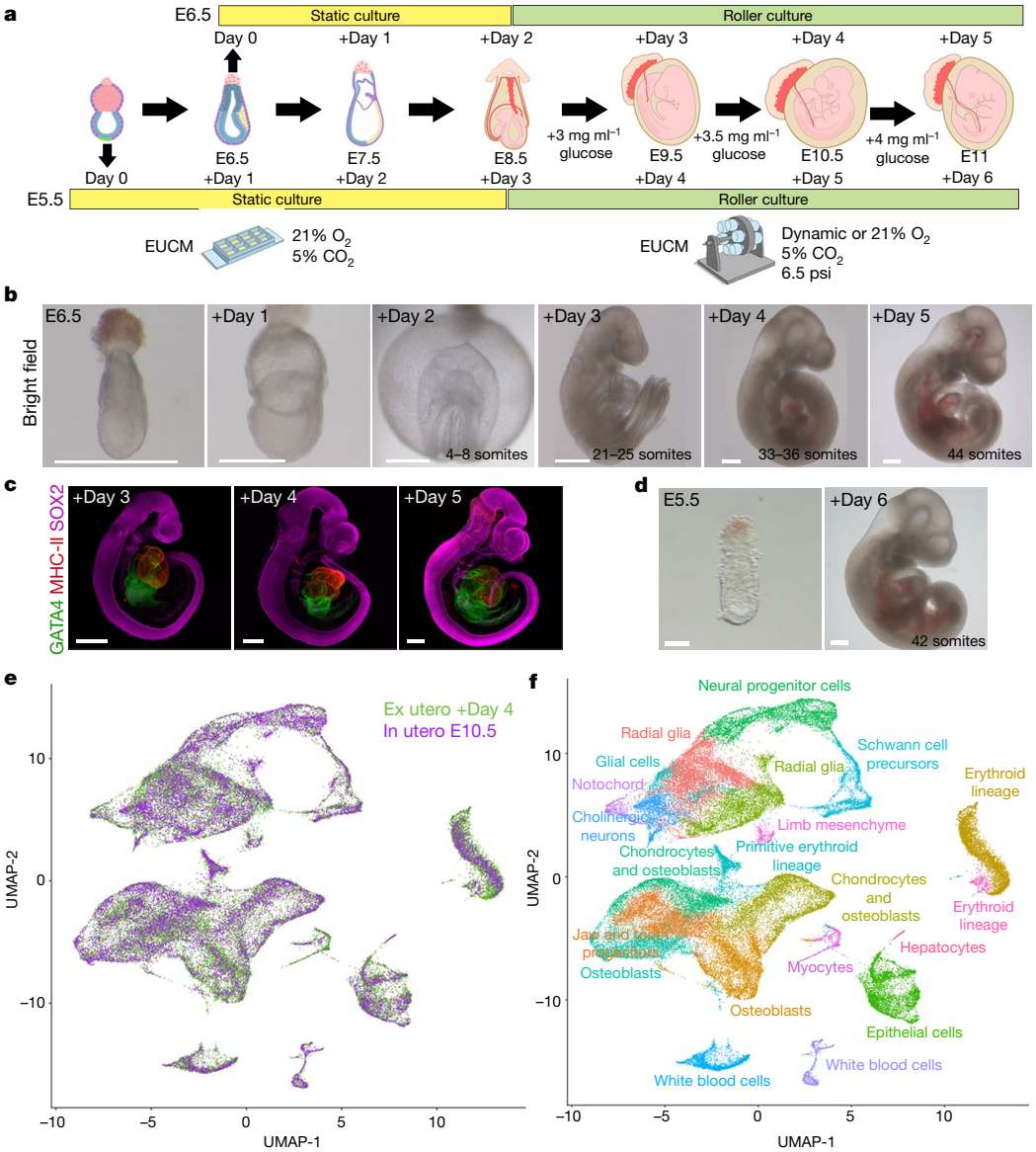

Fig. 3 | Extending the mouse embryo ex utero culture system from pre-gastrulation to advanced organogenesis. a, Schematic protocol for culturing mouse embryos from pre-gastrulation to organogenesis. **b**, Bright-field images of embryos grown for five days ex utero from E6.5 to the 44-somite stage. Embryos cultured beyond day two are shown without the yolk sac. The variation in somite number is indicated. $n \geq 65$ embryos. **c**, Immunostaining of early-gastrulating embryos grown ex utero for 3, 4 and 5 days. Images are representative of at least three biological replicates. **d**, Representative bright-field images of pre-gastrulating E5.5 embryos cultured for 6 days until the 42-somite stage. $n \geq 5$ embryos. Scale bars, 50 µm (E5.5), 500 µm (all others). **e**, Comparative scRNA-seq analysis of E6.5 +Day 4 ex utero embryos (green dots) and equivalent E10.5 embryos developing in utero (purple dots). UMAP plot depicting all cells considered in the analysis ($n = 39{,}374$ ex utero; $n = 24{,}107$ in utero). **f**, Cell lineage annotation of clusters based on the expression of marker genes described in the mouse organogenesis cell atlas[21]. Points are coloured according to their assigned cell cluster.

were located according to their expected expression patterns (Fig. 3c, Extended Data Figs. 7, 9h). HCS could be replaced with serum isolated from human adult blood (HBS) to allow ex utero development until the hindlimb formation stage (44 somites), starting from E6.5 and E7.5 (Extended Data Fig. 10).

We characterized the transcriptional profiles of cells isolated from embryos grown ex utero and in utero matched embryos by scRNA-seq (Extended Data Fig. 8a, b). The cells profiled were grouped into 20 clusters[21] (Extended Data Fig. 8d, f). Our analysis confirmed that the composition of cell transcriptional states in the embryos that had developed ex utero until advanced organogenesis (E6.5 + 4 days) was equivalent to that of their in vivo counterparts (Fig. 3e). The annotated cell clusters identified represent lineage-committed cell types comprising organs and tissues derived from all three germ layers, consistent with advanced organogenesis stages (Fig. 3f). Analysis of differentially expressed genes revealed a high correlation (about 0.9) between ex utero and in utero embryos for all cell states, with the most variable cluster showing only 0.4% (8 out of 2,000) differentially expressed genes (Extended Data Fig. 8g). This minimal difference in blood and cardiac gene expression signature at E10.5 (Extended Data Fig. 8g) could be consistent with early signs of hydrops fetalis in the embryos. Comparison of the relative cell proportions across cell types showed no significant differences in the majority of clusters, while minor differences were found in only three clusters (Extended Data Fig. 8h). Collectively, these results show that embryos developing ex utero from pre-gastrulation stages, by a combination of static and rolling bottle

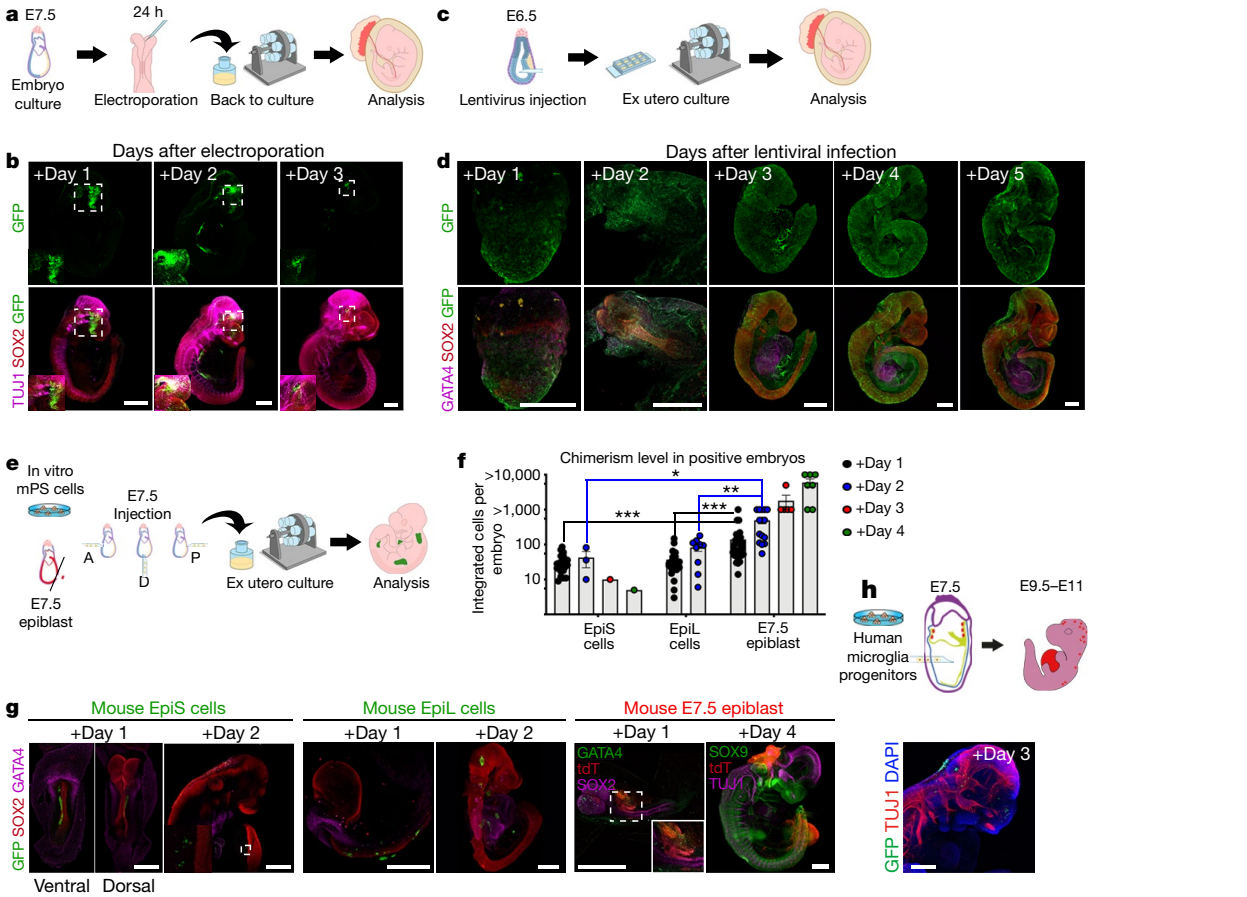

Fig. 4 | Measuring functional outcomes of perturbations introduced into ex utero whole-embryo culture platform. a, Schematic illustration of the ex utero electroporation protocol at E8.5. **b**, Immunofluorescence of electroporated embryos stained for GFP, SOX2 and TUJ1. $n = 17, 15$ and 11 embryos (left to right). **c**, Lentiviral transduction of E6.5 mouse embryos. **d**, GFP, SOX2 and GATA4 immunostaining of E6.5 embryos transduced with GFP using lentivirus and grown ex utero for 1–5 days. $n = 15, 24, 19, 16$ and 20 embryos (left to right). **e**, Generation of post-implantation chimeras by microinjection of primed EpiS cells, EpiL cells and E7.5 in vivo epiblasts. A, anterior; D, distal; P, posterior. **f**, Quantification of GFP$^+$ cells in chimeric embryos. Dots represent individual embryos; data are mean ± s.e.m. Embryos with no contribution are not represented in the graph. Numbers of embryos analysed: EpiS cells, 21, 39, 18, 8; EpiL cells, 22, 9; E7.5 epiblasts, 34, 12, 5, 7 (left to right); Mann–Whitney test. $^{***}P < 0.0001$; $^{**}P = 0.001$; $^{*}P = 0.0025$. **g**, Immunostaining of chimeric embryos injected at E7.5 with GFP–EpiS cells, GFP–EpiL cells or tdTomato (tdT)–E7.5 epiblasts and cultured ex utero for 1–4 days. **h**, Top, generation of human–mouse microglia chimeras. $n = 11$ embryos. Bottom, whole-mount immunostaining of chimeric embryos 3 days after injection. Scale bars, 500 µm.

cultures, are capable of proper symmetry breaking, establishment of the germ layers and embryonic axis, and subsequently differentiation and patterning of tissues and organs without maternal interaction over a period of six days from the symmetric pluripotent epiblast to the advanced organogenesis stages.

Perturbation of post-implantation development

One major advantage of this ex utero culture platform is the ability to apply manipulations in post-implanted mouse embryos, and to follow their effects on the same embryos after several days of further ex utero development. We performed whole-embryo electroporation[4,22] of a fluorescent marker at early E8.5 (before neural tube closure) followed by long-term ex utero culture (72 h). Embryos at E7.5 were dissected and cultured for 24 h. Afterwards, a *GFP* plasmid vector was injected into the neural tube and electroporated to label a population of neural cells. Electroporated embryos were then put back in culture for up to three days (Fig. 4a). Sixty-eight per cent of the embryos developed properly until the hindlimb stage after electroporation (Extended Data Fig. 11a). Cells that expressed GFP were widely distributed in the neural tissues after 1–3 days of culture in 75% of embryos (Fig. 4b, Extended Data Fig. 11b, c).

The ability to perform genetic modifications by lentiviral transduction[23] was also shown in E6.5 embryos by microinjecting lentivirus harbouring a gene encoding enhanced GFP (EGFP) (Fig. 4c). Lentiviral transduction yielded an embryo survival rate similar to that of controls and did not affect morphology or tissue differentiation (Fig. 4d, Extended Data Fig. 11d). After 24 h, GFP was detected throughout the epiblast and extraembryonic tissues, and by the last culture day, GFP expression was extensively spread over the embryo and yolk sac in more than 90% of the embryos (Fig. 4d, Extended Data Fig. 11e).

Next, we harnessed the ex utero culture platform to analyse chimeric mouse embryos obtained after microinjection of primed pluripotent stem cells (PS cells) at post-implantation stages[24]. The ability to evaluate the chimeric potential of primed mouse PS cells has been limited by the lack of protocols that enable transfer of post-implantation embryos in utero or their ex utero culture for prolonged periods, which has now been achieved herein. Thus, we microinjected clusters of GFP-labelled mouse epiblast stem cells (EpiS cells) or epiblast-like stem cells (EpiL cells) into the anterior, distal or posterior epiblast of E7.5 embryos, which were subsequently cultured ex utero (Fig. 4e, Extended Data Fig. 11f, g, i–k). After 24 h, we observed chimerism efficiency of 50–60% for both EpiS cells (27 of 49 embryos) and EpiL cells (44 of 69 embryos) injected into the posterior epiblast, with an estimated number of

transplant-derived cells of 10 to 100 cells distributed along the embryo body axis (Fig. 4f, g, Extended Data Fig. 11i, j), consistent with previous studies[25–27]. Co-immunostaining for SOX2 and GATA4 confirmed that the cells integrated into embryonic tissues (Fig. 4g, Extended Data Fig. 11i). However, the number of EpiS cell-derived GFP$^+$ cells decreased over the subsequent three days and these cells were outcompeted by the cells of the host (Fig. 4f, g, Extended Data Fig. 11i, j). Low integration was also evident when microinjecting EpiS cells and EpiL cells into the anterior and distal epiblasts (Extended Data Fig. 11k). Isogenic naive embryonic stem (ES) cells microinjected into blastocysts that were subsequently transferred and re-isolated at E7.5 and subjected to ex utero culture yielded high-contribution chimeras (Extended Data Fig. 11h). This finding excludes genetic background or ex utero culture as the underlying cause of limited chimeric integration of in vitro-derived primed PS cells. Finally, we injected primed cell clusters isolated directly from tdTomato$^+$ E7.5 embryonic epiblasts into recipient embryos (Fig. 4e). Unlike EpiS cells or EpiL cells, in vivo-derived E7.5 epiblast orthotopic grafts contributed extensively and adequately to chimeric embryos across different tissues (more than 10,000 integrated cells at the last day of culture; Fig. 4f, g, Extended Data Fig. 11j, l). These results suggest that, in relation to their in vivo counterparts, in vitro primed PS cells possess a limited capacity to expand and incorporate into host tissues even when they are injected into post-implantation stages and allowed to undergo advanced organogenesis ex utero.

In toto confocal live imaging can be applied to ex utero developed embryos, as shown by imaging of neural tube closure in tdTomato$^+$ mouse embryos, which were maintained ex utero from E7.5 and subsequently mounted for live confocal imaging at E9.0 to visualize the dynamics of convergence and closure of the neural folds for about 9 h (Extended Data Fig. 11m, Supplementary Video 8). Furthermore, the teratogenic effects of valproic acid on neural tube closure could be recapitulated by supplying this teratogen to the embryo environment ex utero (Extended Data Fig. 11n).

Finally, we derived GFP-labelled primitive microglia progenitors from human PS cells[28] (Extended Data Fig. 12a, b), and microinjected them into mouse embryos at E7.5 followed by ex utero culture (Fig. 4h, Extended Data Fig. 12c). Analysis of integrated human cells revealed that microglia precursors robustly integrated, proliferated and migrated into the host brain (Fig. 4h, Extended Data Fig. 12d–g). The microglial identity of the injected cells was confirmed by the presence of cells that were double-positive for GFP and TMEM119 (Extended Data Fig. 12f). GFP$^+$ human cells were also detected circulating through the yolk sac and yolk sac vessels, indicating that human microglia progenitors can migrate through the mouse embryonic circulation (Extended Data Fig. 12g). These results demonstrate the usability of the platform described herein to shed light on the development of human cells in the context of cross-species embryonic chimeras[29].

Discussion

We have established a robust embryo culture system that faithfully recapitulates mouse in utero post-implantation development from pre-gastrulation to advanced organogenesis stages, enabling the application and monitoring of external and internal manipulations in mouse embryos for up to six days of post-implantation development. The ability to remove a mammalian embryo from the uterine environment and grow it normally under controlled conditions constitutes a powerful tool for characterizing the effects of different perturbations on development during the period from gastrulation to organogenesis, and can be combined with genetic modification, chemical screens, tissue manipulation and microscopy methods. This work establishes that the processes of gastrulation and organogenesis in a mammalian species can be jointly recapitulated entirely and adequately in vitro. The latter findings underscore the self-organizing properties of embryos and set the stage for expanding ex utero embryo research from different mammalian species and from stem cell aggregated synthetic embryos[30].

Online content

Any methods, additional references, Nature Research reporting summaries, source data, extended data, supplementary information, acknowledgements, peer review information; details of author contributions and competing interests; and statements of data and code availability are available at https://doi.org/10.1038/s41586-021-03416-3.

1. Bedzhov, I. & Zernicka-Goetz, M. Self-organizing properties of mouse pluripotent cells initiate morphogenesis upon implantation. *Cell* **156**, 1032–1044 (2014).
2. White, M. D. et al. Long-lived binding of Sox2 to DNA predicts cell fate in the four-cell mouse embryo. *Cell* **165**, 75–87 (2016).
3. New, D. A. T. Whole-embryo culture and the study of mammalian embryos during organogenesis. *Biol. Rev. Camb. Philos. Soc.* **53**, 81–122 (1978).
4. Huang, Q. et al. Intravital imaging of mouse embryos. *Science* **368**, 181–186 (2020).
5. Nicholas, J. S. & Rudnick, D. The development of rat embryos in tissue culture. *Proc. Natl Acad. Sci. USA* **20**, 656–658 (1934).
6. New, D. A. T. & Stein, K. F. Cultivation of mouse embryos in vitro. *Nature* **199**, 297–299 (1963).
7. New, D. A. T., Coppola, P. T. & Terry, S. Culture of explanted rat embryos in rotating tubes. *J. Reprod. Fertil.* **35**, 135–138 (1973).
8. New, D. A. T. Development of explanted rat embryos in circulating medium. *Development* **17**, 513–525 (1967).
9. Beddington, R. S. Induction of a second neural axis by the mouse node. *Development* **120**, 613–620 (1994).
10. Parameswaran, M. & Tam, P. P. L. Regionalisation of cell fate and morphogenetic movement of the mesoderm during mouse gastrulation. *Dev. Genet.* **17**, 16–28 (1995).
11. Tam, P. P. Postimplantation mouse development: whole embryo culture and micro-manipulation. *Int. J. Dev. Biol.* **42**, 895–902 (1998).
12. Cantor, J. R. et al. Physiologic medium rewires cellular metabolism and reveals uric acid as an endogenous inhibitor of UMP synthase. *Cell* **169**, 258–272 (2017).
13. Nagamatsu, G., Shimamoto, S., Hamazaki, N., Nishimura, Y. & Hayashi, K. Mechanical stress accompanied with nuclear rotation is involved in the dormant state of mouse oocytes. *Sci. Adv.* **5**, eaav9960 (2019).
14. Ueda, Y. et al. Intrauterine pressures adjusted by Reichert's membrane are crucial for early mouse morphogenesis. *Cell Rep.* **31**, 107637 (2020).
15. Downs, K. M. & Davies, T. Staging of gastrulating mouse embryos by morphological landmarks in the dissecting microscope. *Development* **118**, 1255–1266 (1993).
16. van Maele-Fabry, G., Delhaise, F. & Picard, J. J. Evolution of the developmental scores of sixteen morphological features in mouse embryos displaying 0 to 30 somites. *Int. J. Dev. Biol.* **36**, 161–167 (1992).
17. Stelzer, Y. et al. Parent-of-origin DNA methylation dynamics during mouse development. *Cell Rep.* **16**, 3167–3180 (2016).
18. McDole, K. et al. In toto imaging and reconstruction of post-implantation mouse development at the single-cell level. *Cell* **175**, 859–876 (2018).
19. Ibarra-Soria, X. et al. Defining murine organogenesis at single-cell resolution reveals a role for the leukotriene pathway in regulating blood progenitor formation. *Nat. Cell Biol.* **20**, 127–134 (2018).
20. Pijuan-Sala, B. et al. A single-cell molecular map of mouse gastrulation and early organogenesis. *Nature* **566**, 490–495 (2019).
21. Cao, J. et al. The single-cell transcriptional landscape of mammalian organogenesis. *Nature* **566**, 496–502 (2019).
22. Saito, T. & Nakatsuji, N. Efficient gene transfer into the embryonic mouse brain using in vivo electroporation. *Dev. Biol.* **240**, 237–246 (2001).
23. Beronja, S., Livshits, G., Williams, S. & Fuchs, E. Rapid functional dissection of genetic networks via tissue-specific transduction and RNAi in mouse embryos. *Nat. Med.* **16**, 821–827 (2010).
24. Morgani, S., Nichols, J. & Hadjantonakis, A. K. The many faces of pluripotency: in vitro adaptations of a continuum of in vivo states. *BMC Dev. Biol.* **17**, 7 (2017).
25. Kojima, Y. et al. The transcriptional and functional properties of mouse epiblast stem cells resemble the anterior primitive streak. *Cell Stem Cell* **14**, 107–120 (2014).
26. Wu, J. et al. An alternative pluripotent state confers interspecies chimaeric competency. *Nature* **521**, 316–321 (2015).
27. Huang, Y., Osorno, R., Tsakiridis, A. & Wilson, V. In vivo differentiation potential of epiblast stem cells revealed by chimeric embryo formation. *Cell Rep.* **2**, 1571–1578 (2012).
28. van Wilgenburg, B., Browne, C., Vowles, J. & Cowley, S. A. Efficient, long term production of monocyte-derived macrophages from human pluripotent stem cells under partly-defined and fully-defined conditions. *PLoS One* **8**, e71098 (2013).
29. Gafni, O. et al. Derivation of novel human ground state naive pluripotent stem cells. *Nature* **504**, 282–286 (2013).
30. Harrison, S. E., Sozen, B., Christodoulou, N., Kyprianou, C. & Zernicka-Goetz, M. Assembly of embryonic and extraembryonic stem cells to mimic embryogenesis in vitro. *Science* **356**, eaal1810 (2017).

Methods

Data reporting

No statistical methods were used to predetermine sample size. Embryos were randomly allocated when placed in the different growth conditions. Other experiments were not randomized. The investigators were not blinded to allocation during experiments and outcome assessment, as there was no relevant scientific reason to do so.

Animals

Female mice (5–8-week-old ICR, C57BL/6 or BDF1) were mated with BDF1 male studs (Harlan). For experiments using transgenic reporter lines mTmG (*Gt(ROSA)26Sor*$^{tm4(ACTB-tdTomato,-EGFP)Luo}$) (Jackson #007576) females were mated with either *Wnt1-Cre* (Jackson #022137) or *Isl1-Cre* (Jackson #024242) males. For live imaging and post-implantation grafting experiments, Ai14(RCL-tdT)-D (B6.Cg-*Gt(ROSA)26Sor*$^{(CAG-tdTomato)Hze}$) (Jackson #007914) mice were crossed with *Stra8-iCre* mice; F1 males were mated with ICR females, and Td-Tomato^{+} embryos were selected. For imprinting experiments, Dlk1-Dio3 IG-DMR-*Snrpn*-GFP (Jackson #030539) males were mated with ICR or C57BL/6 females. Insemination was verified the next morning by the presence of a copulatory plug, and this day was defined as E0.5 days post coitum (dpc). All animal experiments were performed according to the Animal Protection Guidelines of Weizmann Institute of Science, and were approved by the relevant Weizmann Institute IACUC (#01390120-1, 01330120-2, 33520117-2). All mice were housed under standard 12-h light–dark cycle conditions in a specialized and certified animal facility. Additional embryo processing protocols are provided in the Supplementary Methods.

Ex utero whole embryo roller culture and gas regulation module

A step-by-step detailed protocol accompanying this manuscript is available on Protocol Exchange[31]. For cultures starting at E7.5 or later, the embryos were kept on a rotating bottle culture unit inside a Precision Incubator system (BTC01 model with gas bubbler kit by B.T.C. Engineering, Cullum Starr Precision Engineering Ltd) for the duration of culture. A 'rotator' culture method provides a continuous flow of oxygenating gas to cultures in rotating bottles (BTC Rotating Bottle Culture Unit BTC02 model by B.T.C. Engineering, Cullum Starr Precision Engineering Ltd). Culture bottles (Glass Bottles (Small) BTC 03 and Glass Bottles (Large) BTC 04) are plugged into the hollow rotating drum. Oxygenating gas flows along the axis and is distributed to the culture bottles by a baffle plate within the drum. The system maintains a more stable pH than systems with sealed culture bottles. The rotator is supplied complete with gas filter, bubbler and leads by the manufacturer. The BTC Precision Incubator uses a thyristor-controlled heater and high flow-rate fan to give a highly stable and uniform temperature throughout the easily accessible working volume. The incubator has a working volume of 370 × 350 × 200 mm, which is accessed through the hinged Perspex top. The heater element is rated at 750 W. Bung (Hole) BTC 06 is used to seal the bottles and Bung (Solid) BTC 07 is used to seal the drum (B.T.C. Engineering, Cullum Starr Precision Engineering Ltd). The embryo incubator should be shielded from light by external covering with a dark cloth or diaper.

To achieve constant O_2 and CO_2 levels in the culture medium throughout the incubation period, the incubator module was linked to an in-house-designed and customized gas and pressure control unit (model HannaLab1, assembled and maintained by Arad Technologies Ltd). Carbon dioxide and oxygen concentrations are regulated by specific controllers located inside the regulation module. N_2 and CO_2 are then injected into the gas mixer box. The mixing of the gases in the gas box is homogeneous and mixed by a centrifugal blower. A pressure transmitter allows control of the gas pressure between 5 and 10 psi in the gas mixing box (positive pressure over ambient external atmospheric pressure), which is transmitted to the sealed embryo bottle apparatus. The pressure generated by the pressure pump is regulated by setting the adequate voltage on the pressure transmitter (component 10 in Extended Data Fig. 1d, e), set at 5–6 V to obtain pressures of 6–7 psi in the gas mixing box of this specific model. The gases are injected into the incubator at a pressure of about 6–7 psi (which was found to be the optimal level) by a pump that builds pressure. The bubble rate (which indicates the speed of gas flowing into the bottles) can be adjusted as needed by the user by closing or opening the valve on the lid of the water bottle (bubbler unit). Gas flows from the mix box through the inlet into the water bottle, and the speed of gas flowing into the bottle can be controlled with a valve (Extended Data Fig. 1f). Humidified gas circulates to a glass test tube and then to the inside of the bottles in the rotating drum; gas flow speed can be monitored by the rate of bubbles created inside an outlet water-filled test tube. Ideally, the flow of bubbles should be such to allow the formation of individual bubbles at a rate of 1–4 bubbles per second as measured in the outlet water-filled test tube in the right back corner of the incubator. The main components of the system are the following: O_2 and CO_2 controller, pressure pump, vacuum pump, O_2 and CO_2 sensors, power supply, check valve, mix gas box, pressure transmitter, limit flow, adaptor control for gases, 1-µm filters, centrifugal blower (Extended Data Fig. 1). The gas control unit and gas mixing box established here were assembled and maintained by Arad Technologies Ltd. Monthly testing of sensors, tubing and system parameters (pressure and gas concentration) was routinely performed on site by Arad Technologies Ltd to ensure system stability and adequate performance.

Isolation of human umbilical cord blood serum and adult blood serum

For the purpose of this study, healthy pregnant women who were referred to the prenatal clinic at the Rambam Medical Center were asked to give their informed consent to have blood collected from their umbilical cord, as approved by a Rambam Medical Center Helsinki committee (#RMB-0452-15). The source of each collection underwent full anonymization and was not identified by name or other designation, and the extracted serum was used only as described herein. Healthy women over the age of 18 and under 40, who gave their consent and were scheduled for caesarean section delivery by their obstetrician following a prenatal clinic visit, were eligible for cord blood collection. We excluded women who gave birth vaginally as well as women with any chronic illness or active medical conditions, including gestational diabetes or hypertension. On the day of scheduled caesarean delivery and in order to ensure fresh isolation and processing of serum, a team stood by for cord blood collection and serum extraction. Immediately upon delivery of the infant, the umbilical cord was double clamped 5–7 cm from the umbilicus and transected between the clamps. Blood was collected for the purpose of this study, only after the infant had been removed from the field of surgery and umbilical blood had been drawn for clinical tests as needed. To avoid any traces of haemolysis, blood was manually drawn by the obstetric surgeon, using a large-bore 14-gauge needle and a 50-ml syringe, directly from the umbilical vein while the placenta remained in situ. This was done to avoid any coagulation of blood before collection, which could lead to traumatic haemolysis, and also to take advantage of the enhanced blood flow generated by uterine contraction. Next, the collected blood was freshly and quickly distributed into 5-ml pro-coagulant sterile test tubes (Greiner Bio-One, Z Serum Sep Clot Activator, #456005) and cooled to 4 °C for 15 min, to allow full coagulation. Then, coagulated test tubes were centrifuged at 2,500*g* for 10 min in a cooled 4 °C centrifuge. Any tube that showed signs of haemolysis (such as pinkish-red serum) was discarded. The separated serum (yellowish) was collected using a pipette and filtered through a 0.22-µm filter (Nalgene, Ref # 565-0020) and then inactivated in a 55 °C bath for 45 min. The inactivated serum was next distributed into aliquots and placed in a freezer at −80 °C for storage for up to six months. Shipping temperature was kept at −70 °C using dry ice and any thawed serum was not refrozen. Human adult blood serum was

collected from healthy adults and freshly prepared using the same protocol as for umbilical cord blood serum. We noted that in-house freshly prepared human umbilical cord serum and adult human serum gave notably superior results to commercially available ones tested in this study.

E7.5 embryo dissection and ex utero culture

Mouse embryos were obtained from non-hormone primed pregnant mice that were killed by cervical dislocation at E7.5. Subsequently, embryos were dissected out from the uterus in dissection medium pre-equilibrated at 37 °C for 1 h, consisting of DMEM (GIBCO 11880; includes 1 mg/ml D-glucose and pyruvate, without phenol red and without L-glutamine) supplemented with 10% fetal bovine serum (FBS; Biological Industries; 040131A), sterilized with a 0.22-μm filter (JetBiofil; FCA-206-250). The embryos were carefully dissected from the decidua and parietal yolk sac, leaving the intact ectoplacental cone attached to the egg cylinder. In brief, the decidua was isolated from the uterine tissue and the tip of the pear-shaped decidua was cut. The decidua was then opened into halves by introducing the forceps adjacent to the embryo in parallel to its long axis and subsequently opening the forceps. Afterwards, the embryo was grasped from the decidua and the parietal yolk sac was peeled off the embryo using two forceps. Embryo dissection was performed on a microscope equipped with a Tokai Hit thermo plate at 37 °C, within a maximum of 30 min to avoid affecting the developmental potential of the embryo. Embryos in the neural plate/early head-fold stage that showed no evidence of damage in the epiblast were selected for culture. The developmental stage of the embryos was determined as described[15]. EUCM consisted of 25% DMEM (GIBCO 11880; includes 1 mg/ml D-glucose and pyruvate, without phenol red and without L-glutamine) supplemented with 1× glutamax (GIBCO, 35050061), 100 units/ml penicillin and 100 μg/ml streptomycin (Biological Industries; 030311B) and 11 mM HEPES (GIBCO, 15630056), plus 50% rat serum (rat whole embryo culture serum, ENVIGO Bioproducts B-4520) and 25% HCS prepared in-house. DMEM (GIBCO 11880) supplemented with glutamax, penicillin/streptomycin and HEPES was stored at 4 °C in aliquots and used within 2 months. Rat serum was stored at −80 °C, heat-inactivated at 56 °C for 30 min and filtered through a 0.22-μm PVDF filter (Millipore; SLGV033RS) before use. HCS was collected at Rambam Medical Center in Haifa, Israel, and stored as heat-inactivated and filtered aliquots at −80 °C. HCS was freshly thawed and used immediately before experimentation. HCS could be replaced by freshly collected HBS. HBS was collected and stored as heat-inactivated and filtered aliquots at −80 °C. Rat serum, HCS and HBS could be thawed and refrozen once. Culture medium was pre-heated for at least one hour by placing it inside a glass bottle on the rotating culture. Immediately after dissection, groups of 5–6 embryos were transferred into glass culture bottles (B.T.C. Engineering, Cullum Starr Precision Engineering Ltd) containing 2 ml EUCM. The bottles were placed on a rotating bottle culture system, rotating at 30 rpm at 37 °C, and continuously gassed with an atmosphere of 5% O_2, 5% CO_2 at 6.5 psi. After 24 h, groups of three embryos were moved to a new bottle containing 2 ml freshly prepared medium supplemented with an extra 3 mg/ml D-glucose (J.T. Baker) (in addition to the 1 mg/ml glucose found in the base DMEM), and a gas mixture of 13% O_2, 5% CO_2. At 48 h of culture, embryos were transferred to a new bottle (two embryos per bottle) with fresh medium supplemented with 3.5 mg/ml glucose and cultured a gas atmosphere of 18% O_2 and 5% CO_2. After 72 h of culture, each embryo was moved to an individual bottle with 1.5 ml fresh medium plus 4 mg/ml glucose, with a gas supply of 21% O_2 and 5% CO_2. For medium exchange, culture medium was pre-heated for at least one hour by placing it inside a glass bottle on the rotating culture with an adequate gas atmosphere depending on the stage of the cultured embryos. Embryos were imaged each day using a Discovery V.20 stereoscope (Carl Zeiss). For paternal imprinting experiments, littermate embryos lacking the reporter allele were used as negative controls. For teratogenic experiments, 1 mM valproic acid (Sigma-Aldrich, P4543) diluted in water was added directly to the culture medium during pre-heating.

During the process of media optimization, to reach a meaningful conclusions regarding each serum or tissue culture supplement, at least three different lots (batches) of reagent from the same vendor were used. The following supplements were tested: KSR (KnockOut Serum Replacement, GIBCO 10828010), HPLM (human plasma-like medium, kindly provided by J. Cantor[12]), N-2 Supplement (GIBCO, 17502048), and B-27 Supplement (GIBCO, 17504044).

Ex utero culture of E5.5 and E6.5 embryos

Cultures starting with pre-gastrulation (E5.5) and early gastrulation (E6.5) embryos were done in static culture conditions until the early somite stage. Embryos were dissected out of the uterus as described above and individual embryos were transferred into each well of an 8-well glass bottom/ibiTreat μ-plate (iBidi; 80827/80826) filled with 250 μl EUCM. Medium was pre-heated for an hour in an incubator with 5% CO_2 at 37 °C. Pre-primitive streak stage embryos (distal and anterior visceral endoderm stage) were chosen for culture in the case of E5.5, and early-primitive streak stage embryos were selected for cultures beginning at E6.5. Only embryos with no evident damage and without Reichert's membrane were cultured. The total volume of medium was replaced every 24 h. Embryos were transferred into the rotating culture at the 4–7-somite stage (three days for cultures started at E5.5 and two days for cultures started at E6.5) using the same conditions described previously for E8.5, with the difference that embryos were maintained in a constant atmosphere of 21% oxygen and 5% CO_2. Transfer of the embryos at earlier or later somite stages resulted in failure of further development. Dynamic oxygen conditions yielded slightly less efficiency for expanding E6.5–E11 than using constant 21% O_2 (Extended Data Fig. 6a, b). This difference could result from oxygen diffusion in static conditions being less efficient than in roller conditions, and that might be why higher oxygen is needed to be delivered in protocols that include static conditions. For testing static cultures using higher gas pressures we used the Avatar (XCell Biosciences) pressurized incubator at 2.5 and 5 psi in 21% O_2. HCS could be replaced by HBS with a minor decrease in survival efficiency. For live imaging methodology, see Supplementary Methods.

Whole-mount immunostaining of E5.5–E8.5 mouse embryos

Embryos grown ex utero and in utero were dissected, removing the Reichert's membrane for E6.5–E7.5 embryos, or the yolk sac and amnion for E8.5 embryos, washed once with 1× PBS, then transferred to iBidi glass bottom 8-well slides (iBidi) and fixed with 4% PFA EM grade (Electron Microscopy Sciences, 15710) in PBS at 4 °C overnight. Embryos were then washed in PBS for 5 min three times, permeabilized in PBS with 0.5% Triton X-100/0.1 M glycine for 30 min, blocked with 10% normal donkey serum/0.1% Triton X-100 in PBS for 1 h at room temperature (RT), and incubated overnight at 4 °C with primary antibodies, diluted in blocking solution. Next, embryos were rinsed three times for 5 min each in PBS/0.2% TritonX-100, incubated for 2 h at room temperature with secondary antibodies diluted 1:200 in blocking solution (all secondary antibodies were from Jackson ImmunoResearch), counterstained with DAPI (1 μg/ml in PBS) for 10 min, and washed with PBS for 5 min three times. If necessary, yolk sacs separated from the embryos were fixed and stained following this protocol. For details of primary antibodies and imaging see Supplementary Methods.

iDISCO immunostaining of E9.5–E11.5 mouse embryos

Clearing of embryos from E9.5 to E11.5 was performed as described[32] with some modifications. After blocking, embryos were incubated with primary antibodies diluted in PBS/0.2%Tween-20 with 10 μg/ml heparin (PTwH)/5% DMSO/3% donkey serum at 37 °C (E9.5/E10.5, 24 h; E11.5, 48 h (72 h for SOX17 and FOXA2 antibodies)). Afterwards, samples were washed in PTwH for 24 h (15 min, 30 min, 1 h, 2 h, and overnight washes),

and incubated with adequate secondary antibodies (1:200) diluted in PTwH/3% donkey serum at 37 °C for 48 h. For human cell-specific NUMA staining, donkey anti-rabbit biotin and streptavidin-Cy3 (each incubated overnight) were used for signal enhancement. Next, embryos were incubated for 30 min with DAPI (1 µg/ml) diluted in PTwH, washed in PTwH for one day (5 min, 15 min, 30 min, 1 h, 2 h, and overnight washes) and dehydrated in a methanol/H_2O series (1 h each), and then incubated overnight in 100% methanol. Embryos were incubated in 66.6% DCM/33.3% methanol on a shaker for 3 h, followed by 100% DCM (Sigma; 270997) for 5 min, and finally cleared and stored in benzyl ether (Sigma; 108014). For details of primary antibodies and imaging see Supplementary Methods.

Statistical analysis

All statistical analyses were performed using GraphPad Prism 8 software (La Joya, California). Data on graphs are shown as mean ± s.e.m. of a minimum of two independent experiments, unless otherwise stated. A Kolmogorov–Smirnov test was performed to check normal distribution of data before each statistical test. Significant differences between two samples were evaluated by unpaired two-sided Student's *t*-test if data were normally distributed or Mann–Whitney test for non-normally distributed data. $P < 0.05$ was considered as statistically significant.

Single-cell RNA-seq

Ex utero cultured embryos dissected from the maternal uterus at E6.5 were sequenced at two time points (after two days and four days of culture). In utero and ex utero developmentally matched embryos were dissociated using Trypsin–EDTA solution A 0.25% (Biological Industries; 030501B) for 10 min and 15 min, respectively, at 37 °C. E8.5 embryos were processed including the yolk sac but after removal of the ectoplacental cone, and for E10.5 only the embryo proper was processed with the extraembryonic membranes removed. Trypsin was neutralized with medium including 10% FBS and cells were washed and resuspended in 1× PBS (calcium- and magnesium-free) with 400 µg/ml BSA. The cell suspension was filtered with a 100-µm cell strainer to remove cell clumps. A cell viability percentage higher than 90% was determined by trypan blue staining. Cells were diluted to a final concentration of 1,000 cells per µl. Each group of embryos at E8.5 (four ex utero and four in utero) was run into two independent channels of the Chromium 10x Genomics chip, the first channel containing an independent embryo while the second channel consisted of three embryos pooled together. All E10.5 embryos (seven ex utero and five in utero) were run as independent samples. scRNA-seq libraries were generated using the 10x Genomics Chromium v3 system (5,000-cell target cell recovery) and sequenced on an Illumina NovaSeq 6000 platform according to the manufacturer's instructions.

Single cell RNA-seq data processing

10x Genomics data analysis was performed using Cell Ranger 3.1.0 software (10x Genomics) for pre-processing of raw sequencing data, and Seurat 3.0[33,34] for downstream analysis. The mm10-3.0.0 gene set downloaded from 10x was used for gene reference requirements. To filter out low-expressing single cells, possible doublets produced during the 10x sample processing, or single cells with extensive mitochondrial expression, we filtered out cells with under 200 expressing genes, over 4,000 expressing genes and over 15% or 10% mitochondrial gene expression in E8.5 (day 2) and E10.5 (day 4), respectively. Filtering from E8.5 and E10.5 (accumulated samples of in utero and ex utero) reduced the cell count from 16,317 to 10,707 cells and from 64,543 to 63,481 cells, respectively. Seurat integrated analysis and anchoring of all individual samples was performed and then normalized by log-normalization using a scale-factor of 10,000. The top 2,000 variable genes were identified by the variance stabilizing transformation method, and subsequently scaled and centred. Principal components analysis was performed for dimensional examination using the 'elbow' method. The first 15 dimensions showed the majority of data variability. Therefore, UMAP dimensional reduction was performed on the first 15 dimensions in all samples. The parameters for fold-change-threshold used for identification of differentially expressed genes were log(0.25) and min.pct = 0.25 for embryos at both E8.5 and E10.5. For cluster annotation, we used the area under the curve (AUC) methodology to identify the enrichment of each annotated gene-set to each individual single cell. The annotations were based on published gene annotations[19] for E8.5 (day 2) embryos and on the Mouse Organogenesis Cell Atlas[21] for E10.5 (day 4) embryos, and performed using the R package AUCELL 1.10.0[35], using parameters: aucMaxRank = 100 (5% of the total gene count) under the AUCell_calcAUC function. Each cell was then annotated to a single tissue based on its highest AUC score prediction. Each tissue was then cross-tabulated with each cluster to assess cluster–tissue overlap, and additionally normalized by *z*-score and ranged to 0–1 for plotting purposes. Next, to evaluate the probability of a certain cluster being enriched in a certain tissue, we used the annotated AUC predictions of each cell to a tissue to compare to our observed cluster annotation of each cell, thus producing a *P* value based on Mann–Whitney *U* statistics. This was calculated using the R package roc.area v1.42 (CRAN.R-project.org). Integration of both the predicted annotation overlap and its statistical enrichment to each cluster resulted in a single predicted tissue per cluster. Differentially expressed genes (DEGs) of compatible clusters between in utero and ex utero embryos were identified using parameters: fold-change-threshold of log(0.5) and with min.pct = 0.25. DEGs with significant values were also enriched using the gene ontology database via R package limma 3.42.2[36] using function 'goana'. To assess significant changes in the proportional size of each cluster between in utero and ex utero at E10.5, a *t*-test of the proportional size of each cluster was evaluated and corrected using Bonferroni correction, comparing the two groups.

Reporting summary

Further information on research design is available in the Nature Research Reporting Summary linked to this paper.

Data availability

Bulk and single-cell RNA-seq data have been deposited in the Gene Expression Omnibus (GEO) database under accession number GSE149372. Source data are provided with this paper.

31. Aguilera-Castrejon, A. & Hanna, J. H. Highly conducive ex utero mouse embryogenesis from pre-gastrulation to late organogenesis. *Protoc. Exch*. https://doi.org/10.21203/rs.3.pex-1372/v1 (2021).
32. Renier, N. et al. iDISCO: a simple, rapid method to immunolabel large tissue samples for volume imaging. *Cell* **159**, 896–910 (2014).
33. Stuart, T. et al. Comprehensive integration of single-cell data. *Cell* **177**, 1888–1902 (2019).
34. Butler, A., Hoffman, P., Smibert, P., Papalexi, E. & Satija, R. Integrating single-cell transcriptomic data across different conditions, technologies, and species. *Nat. Biotechnol*. **36**, 411–420 (2018).
35. Aibar, S. et al. SCENIC: single-cell regulatory network inference and clustering. *Nat. Methods* **14**, 1083–1086 (2017).
36. Ritchie, M. E. et al. limma powers differential expression analyses for RNA-sequencing and microarray studies. *Nucleic Acids Res*. **43**, e47 (2015).

Acknowledgements This work was funded by Pascal and Ilana Mantoux; the European Research Council (ERC-CoG-2016 726497-Cellnaivety); the Flight Attendant Medical Research Council (FAMRI); an Israel Cancer Research Fund (ICRF) professorship; BSF; the Helen and Martin Kimmel Institute for Stem Cell Research; the Helen and Martin Kimmel Award for Innovative Investigation; the Israel Science Foundation (ISF); Minerva; the Sherman Institute for Medicinal Chemistry; the Nella and Leon Benoziyo Center for Neurological Diseases; the David and Fela Shapell Family Center for Genetic Disorders Research; the Weizmann–U. Michigan program; the Kekst Family Institute for Medical Genetics; the Dr. Beth Rom-Rymer Stem Cell Research Fund; the Edmond de Rothschild Foundations; the Zantker Charitable Foundation; and the Estate of Zvia Zeroni. We thank O. Reiner and T. Sapir for help with mouse embryo electroporations; the Crown Genomics institute of the Nancy and Stephen Grand Israel National Center for Personalized Medicine at the Weizmann Institute for support with scRNA-seq; and the Weizmann Institute management and board for providing critical financial and infrastructural support. We dedicate this paper to the memories of R. Massarwa and H. Garty.

Author contributions A.A.-C. designed and conducted most of the wet lab, embryology, sequencing and imaging experiments, established the ex utero culture protocol and co-wrote the manuscript. B.O. conducted embryo injections, performed human microglia cultures and generated human–mouse chimeras, assisted in culture condition testing and processed cryosections. T.S. conducted bioinformatics analysis with N.N. supervising. R.M. helped to reproduce previously published protocols for ex utero culture and taught immunohistochemical protocols to our team. I.M. submitted Helsinki approval, collected cord blood and calibrated human cord serum production. N.G. recruited donors and performed cord blood extraction during caesarean sections. C.I. and S.S. assisted with human cord serum production. S.T. generated lentiviruses and assisted in embryo immunostaining and lentiviral infection of embryos. J.B., D.S. and S.V. performed tissue culture and bulk RNA sequencing of mouse pluripotent stem cells. V.C., S.A. and L.L. assisted with embryo immunostaining. N.L. performed characterization of cultured cells by qPCR. M.A. and H.K.-S. assisted with library preparation and single-cell RNA sequencing. Y.A. assisted with light sheet microscopy and live imaging. Y.R., S.C. and Y.S. generated tdTomato reporter embryos and assisted with allele imprinting experiments. M.Z. assisted with embryo injections. R.S. assembled and maintained the gas-pressure regulator module. J.H.H. conceived the idea for this project, conceptually designed the gas regulator module, established the ex utero culture protocol, supervised execution of experiments and adequate analysis of data, and wrote the manuscript.

Competing interests J.H.H is an advisor to Biological Industries Ltd, and submitted a patent application that covers the roller and static culture conditions described herein (filed by J.H.H. and the Weizmann Institute of Science). R.S. is CEO of Arad Technologies Ltd. All other authors declare no competing interests.

Additional information

Supplementary information The online version contains supplementary material available at https://doi.org/10.1038/s41586-021-03416-3.

Correspondence and requests for materials should be addressed to A.A.-C., I.M. or J.H.H.

Peer review information *Nature* thanks Hiromitsu Nakauchi, Magdalena Zernicka-Goetz and the other, anonymous, reviewer(s) for their contribution to the peer review of this work.

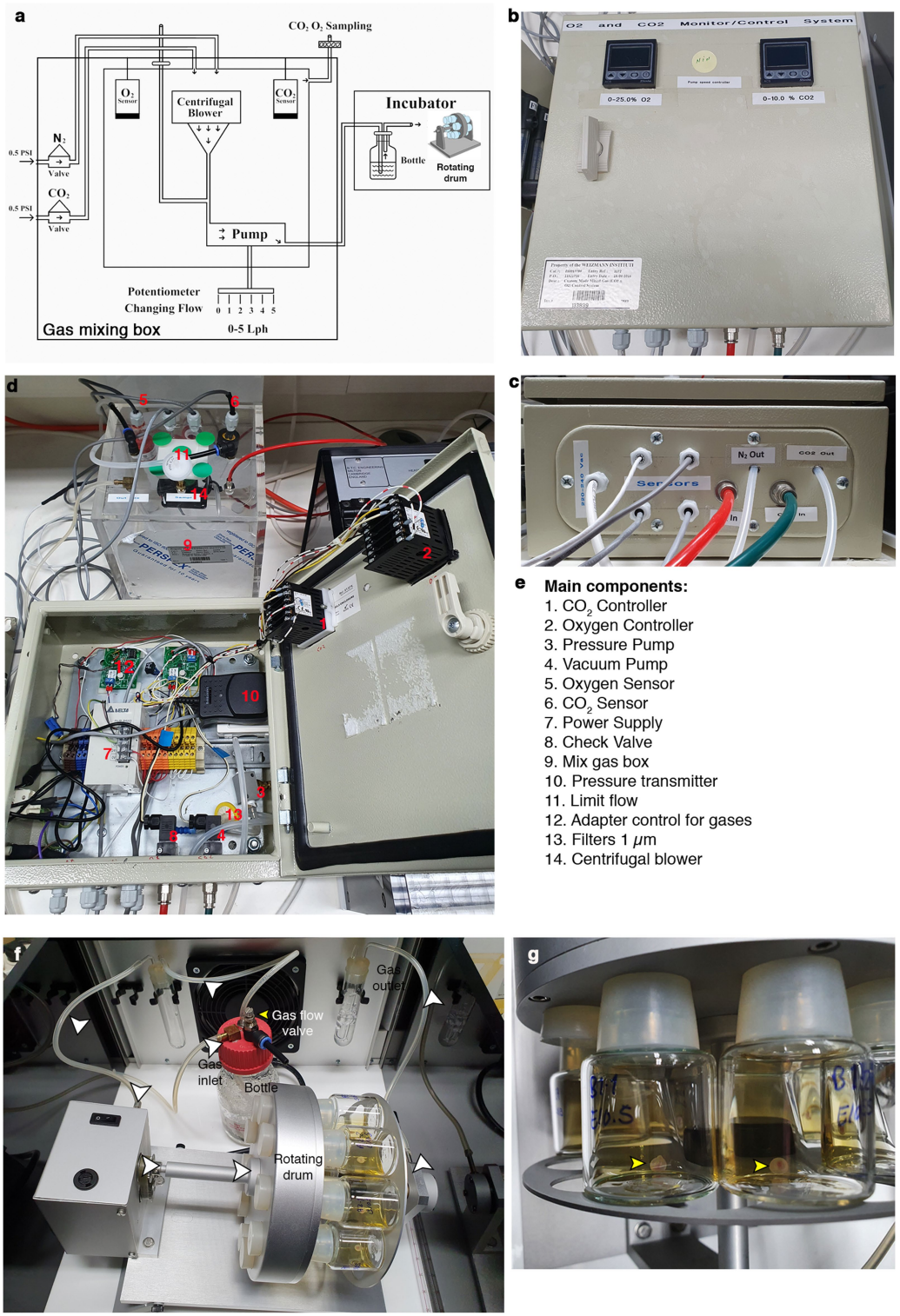

Extended Data Fig. 1 | Optimized gas-regulating module for roller culture incubators. a, Diagram depicting the configuration of the gas-mixing box for gas concentration and pressure regulation. N_2 and CO_2 enter the gas-mixing box and are mixed by a centrifugal blower. Gases are then injected into a water bottle inside the incubator by a pressure pump that allows control of the gas pressure in the gas-mixing box that is transmitted to the sealed embryo bottle apparatus. The voltage on the pressure transmitter controls the pressure generated by the pressure pump in the gas mixing box. Lph, litres per hour. **b**, **c**, Top and front views of the gas controller module. **d**, **e**, Picture displaying the localization of the main components in the gas regulation module (**d**; listed in **e**). **f**, Interior of the precision incubator system (by B.T.C. Engineering, Cullum Starr Ltd) showing the direction of the gas flow (white arrowheads). **g**, Image of day 3 (E10.5) embryos cultured in rotating bottles (yellow arrowheads).

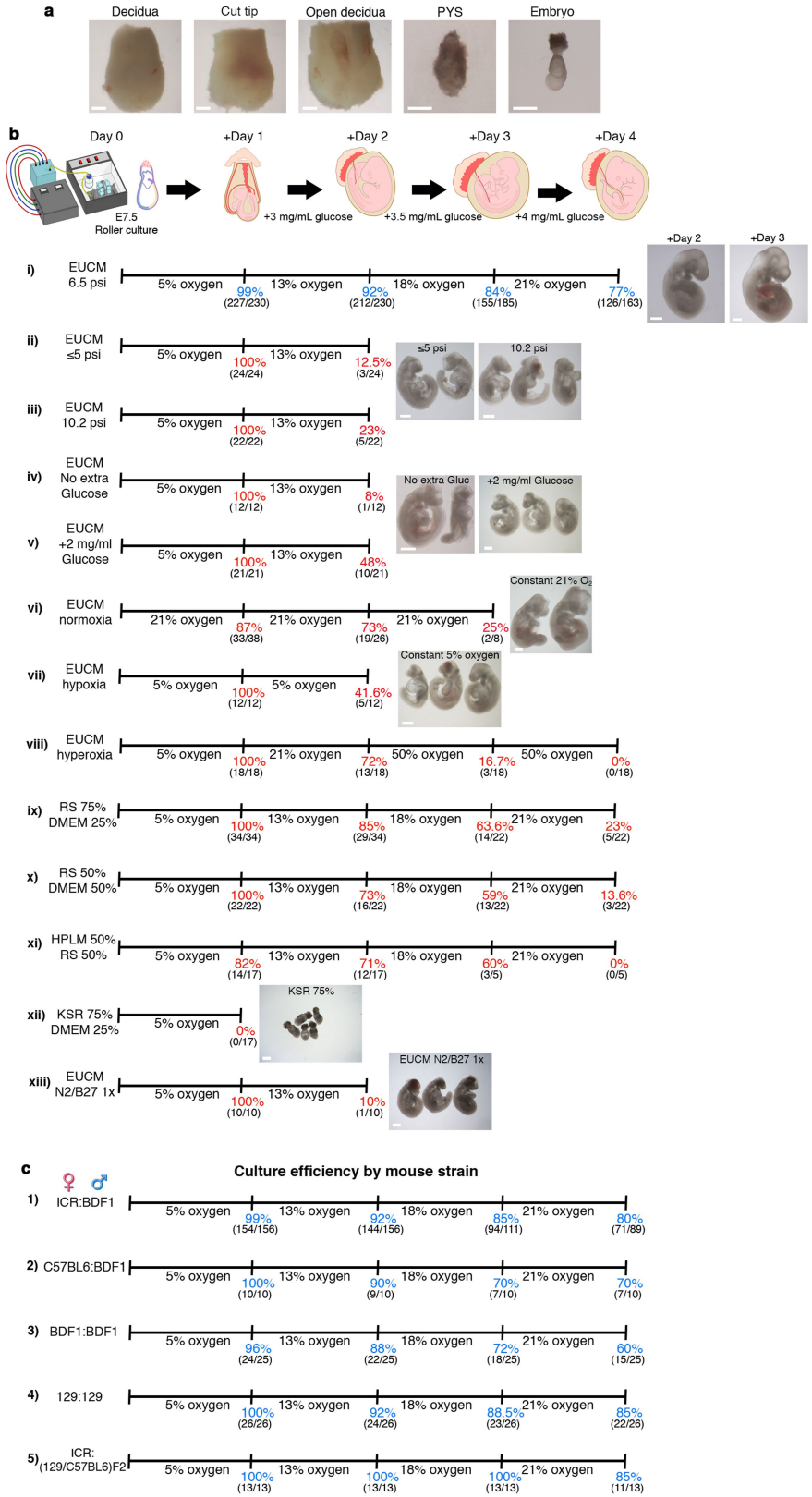

Extended Data Fig. 2 | Establishment and optimization of a mouse embryo ex utero culture from late gastrulation (E7.5) until advanced organogenesis (E11). a, E7.5 embryo dissection overview (see Methods). **b**, Percentage of normally developed embryos under different gas pressures and glucose or oxygen concentrations. Blue numbers indicate the conditions that yielded the highest efficiency of embryo survival. Values in parentheses denote the number of embryos assessed per condition at every sampled time point. Embryos that were dissected, fixed or moved to other conditions are subtracted from the total. Representative bright-field images of embryos cultured under certain conditions are shown to the right. **c**, Efficiency of normal embryonic development evaluated in different mouse genetic backgrounds. Parental mouse lines are indicated on the left (female: male). Values in parentheses show the numbers of embryos evaluated. PYS, parietal yolk sac; RS, rat serum. Scale bars, 500 µm.

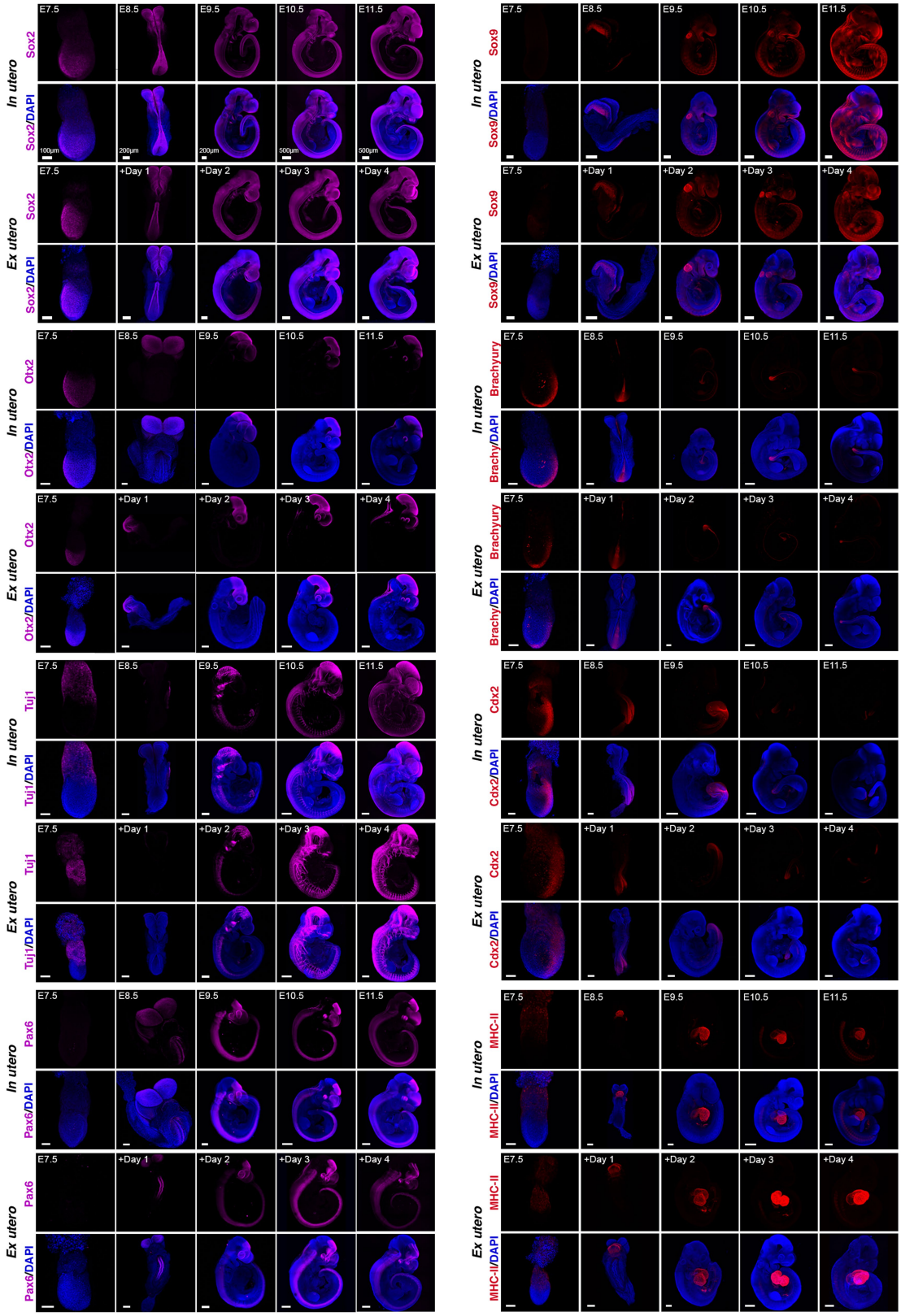

Extended Data Fig. 3 | Spatio-temporal expression patterns of ectoderm- and mesoderm-related lineage markers are recapitulated in ex utero cultured embryos. Maximum intensity projections of embryos developed in utero and ex utero, fixed and immunostained for SOX2, OTX2, TUJ1, PAX6, SOX9, Brachyury, CDX2 and MHC-II (myosin heavy chain-II) at the indicated stages. Blue, DAPI. Images are representative of a minimum of three biological replicates. Scale bars, 100 µm (E7.5), 200 µm (E8.5, E9.5), and 500 µm (E10.5, E11.5).

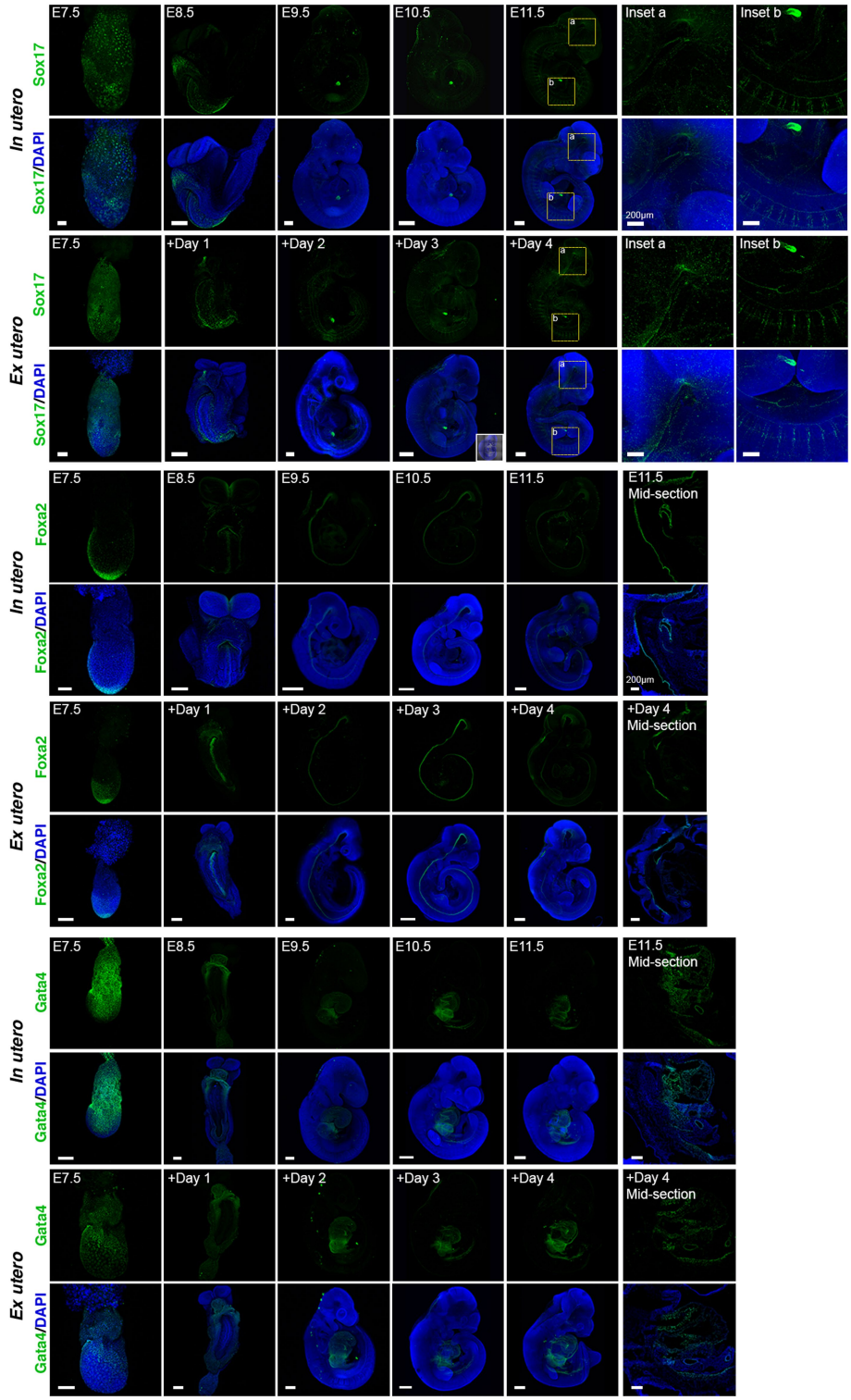

Extended Data Fig. 4 | In vivo spatio-temporal expression patterns of endoderm-related lineage markers are recapitulated in cultured embryos. Maximum intensity projections of embryos developed in utero and ex utero, fixed and immunostained for SOX17, FOXA2 and GATA4 at the indicated stages. Blue, DAPI. For SOX17, insets are enlargements of the dashed boxes. Representative immunohistochemistry (mid-section, sagittal plane) images are shown for FOXA2 and GATA4 at the last time point (far-right panels). Images represent a minimum of three biological replicates. Scale bars, 100 µm (E7.5), 200 µm (E8.5, E9.5), and 500 µm (E10.5, E11.5).

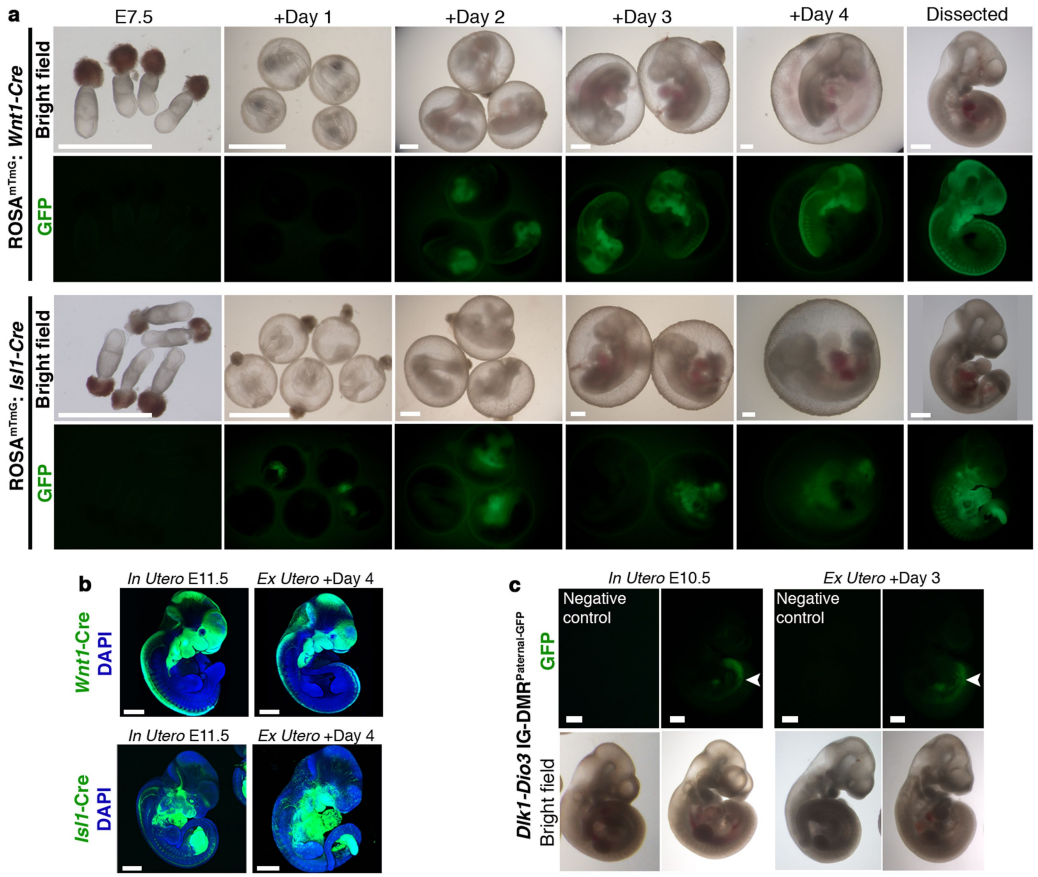

Extended Data Fig. 5 | Ex utero culture of GFP-reporter transgenic embryos. a, Bright-field and GFP fluorescence images of ex utero embryos in culture at the specified times expressing the GFP reporter following activation by *Wnt1-Cre* and *Isl1-Cre* lineage-specific reporter alleles. $n = 7$ and 10 embryos for *Wnt1-Cre* and *Isl1-Cre*, respectively. Embryos dissected out of the yolk sac at +Day 4 are shown in the far-right panel. Scale bars, 500 µm. **b**, Representative confocal images of in utero E11.5 and ex utero +Day 4 transgenic mouse embryos expressing GFP following activation by *Wnt1-Cre* and *Isl1-Cre* reporter alleles. Scale bars, 1 mm. **c**, GFP fluorescence and bright-field images of in utero E10.5 and ex utero +Day 3 IG-DMR–GFP reporter embryos. $n = 7$ in utero; $n = 7$ ex utero. Scale bars, 500 µm.

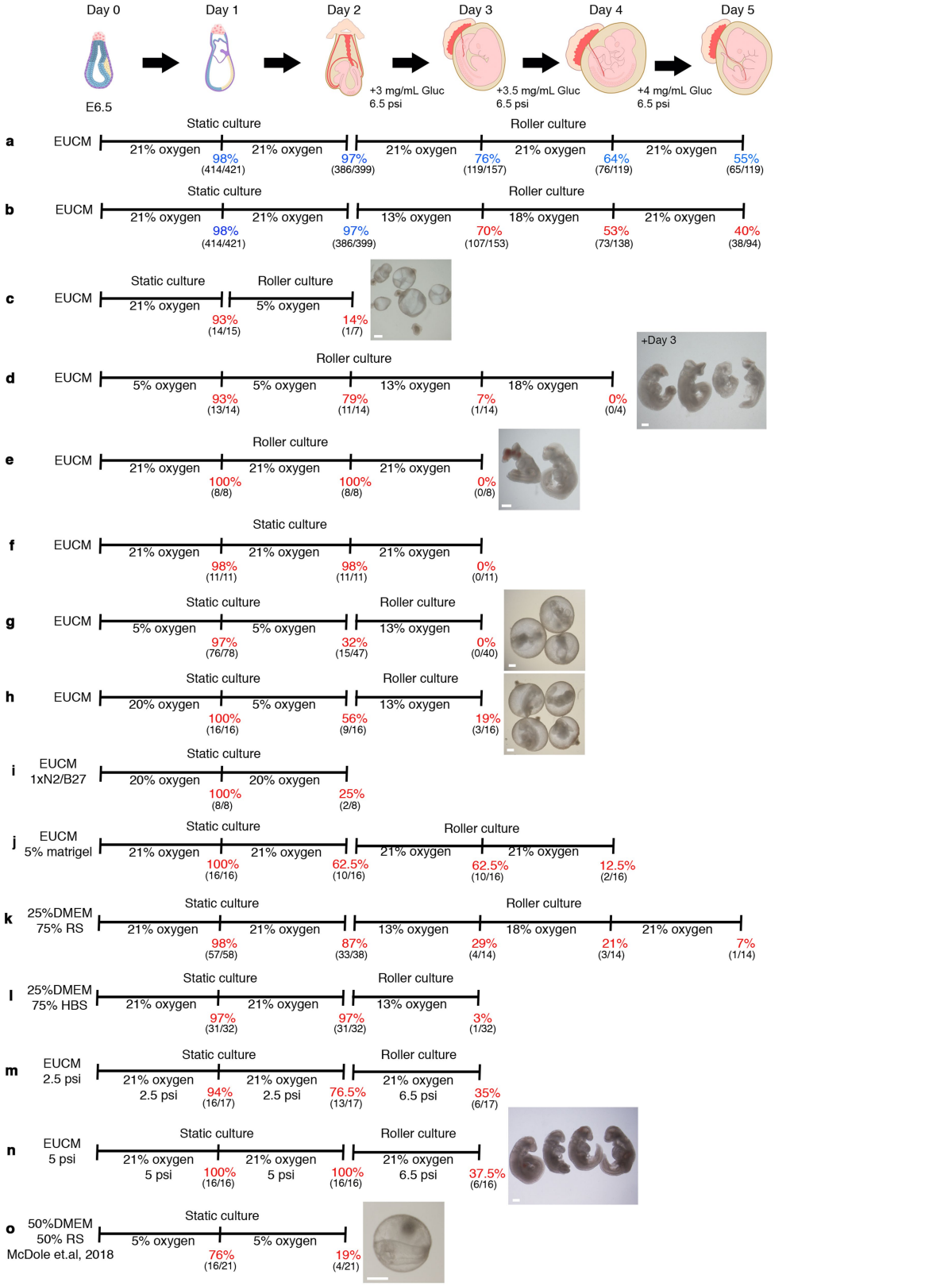

Extended Data Fig. 6 | Devising a platform for culturing mouse embryos from the onset of gastrulation until advanced organogenesis. **a**–**o**, Schematic protocols indicating the percentages of E6.5 embryos that had developed properly per day in each condition. The medium composition, static or roller culture, and oxygen concentration are specified for each protocol. Values in parentheses denote the number of embryos evaluated per condition. Embryos that were dissected, fixed or moved to other conditions are subtracted from the total. Representative bright-field images of embryos cultured under certain conditions are shown to the right. Numbers in blue indicate the protocol that yielded the highest efficiency of embryo survival and was subsequently used throughout the study. Scale bars, 500 µm.

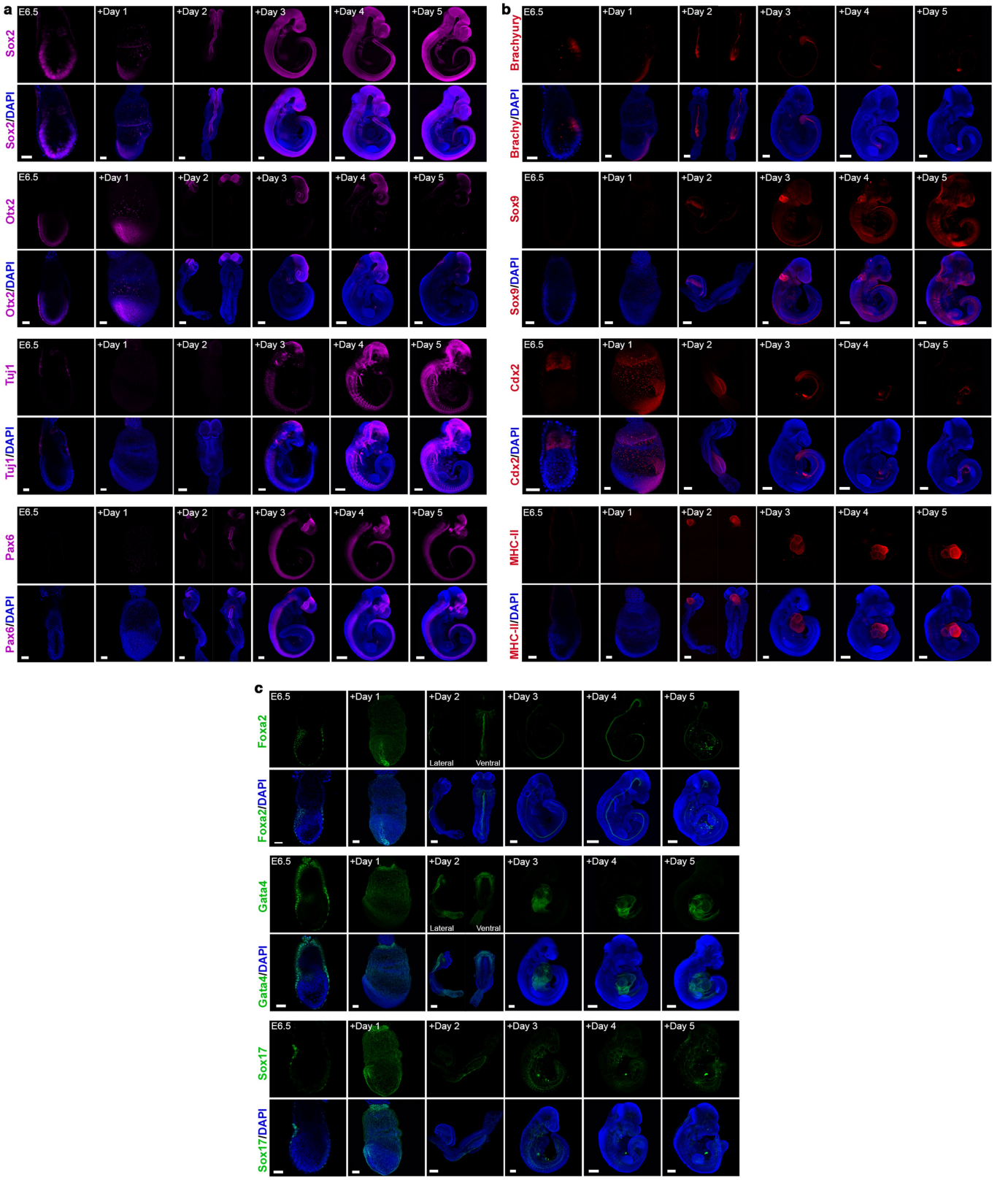

Extended Data Fig. 7 | Embryos grown ex utero since early gastrulation recapitulate the spatio-temporal expression profiles of lineage markers seen in utero. a–**c**, Maximum intensity projections of embryos developed ex utero, fixed, and immunostained for eleven specific markers at the indicated time points. Blue, DAPI. Images are representative of a minimum of three biological replicates. Scale bars, 50 µm (E6.5), 100 µm (+Day 1), 200 µm (+Day 2/3), 500 µm (+Day 4/5).

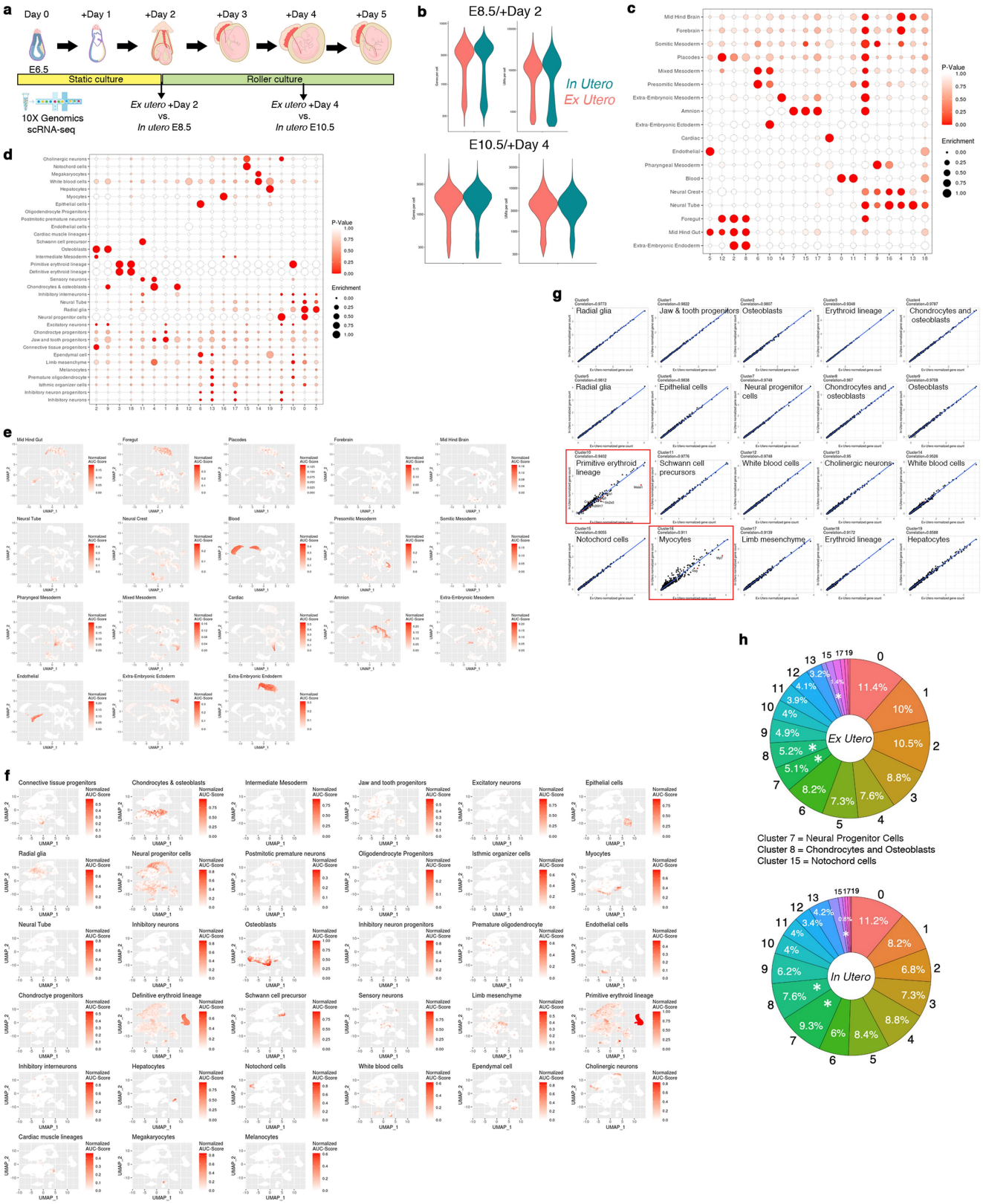

Extended Data Fig. 8 | See next page for caption.

Extended Data Fig. 8 | Single-cell transcriptomic analysis of ex utero +Day 2 and +Day 4 cultured embryos compared to in utero E8.5 and E10.5 embryos. a, Schematic illustration of the embryo culture protocol and sequenced time points. Early-gastrulating (E6.5) embryos grown ex utero were processed for 10x Genomics scRNA-seq after 2 or 4 days of culture. **b**, Violin plot indicating the number of unique molecular identifiers (UMIs) and genes obtained per condition at each time point. E8.5, median of 9,787 UMIs and 2,989 genes detected per cell; E10.5, median of 4,795 UMIs and 1,789 genes detected per cell. **c**, **d**, Lineage annotation at culture days +2 (**c**) and +4 (**d**). Dot plots illustrating the area under the curve (AUC) enrichment value of overlapping cells across clusters and tissue lineages. Circle size denotes the magnitude of enrichment. Colours indicate *P* value (calculated from AUC). **e**, **f**, UMAP-based plots illustrating the normalized AUC assigned value of all individual cells for each lineage at culture days +2 (**e**) and +4 (**f**). **g**, Correlation of gene expression of the top 2,000 most variable genes per cluster between in utero E10.5 and ex utero +Day 4 embryos. Differentially expressed genes are named and shown as red dots. Clusters with the highest number of variable genes (range of 2–8 genes only per cluster) are encased in a red box. **h**, Pie charts depicting the proportional abundance of each cell cluster in both in utero and ex utero developed embryos at +Day 4/E10.5. Asterisks denote clusters with statistically significant differences between the two groups. Cluster 7, $P = 0.004$; cluster 8, $P = 0.009$; cluster 15, $P = 0.001$.

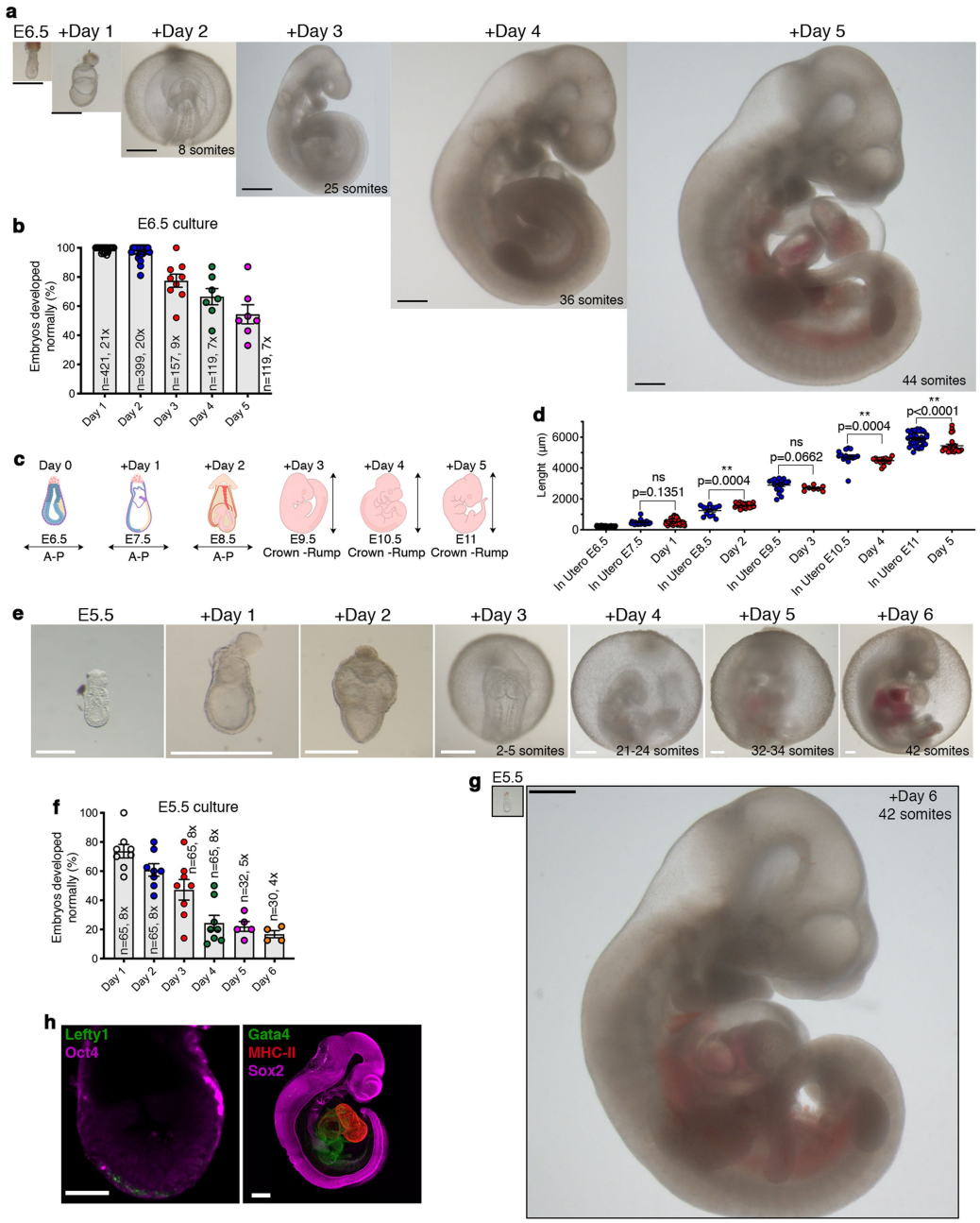

Extended Data Fig. 9 | Changes in morphology and size in embryos developing ex utero from pre-gastrulation to the hindlimb formation stage. a, Proportional increase in size of ex utero embryos grown from the onset of gastrulation (E6.5) to the 44-somite stage. Representative bright-field images of embryos cultured for 5 days are shown at each specific stage. Embryos without yolk sac are shown from day 3 to day 5. $n \geq 119$. **b**, Percentages of normal embryos in cultures started at E6.5. **c**, Diagram depicting the embryonic axis measured at each stage (length of the antero-posterior axis (A-P) for E6.5 to E8.5 and crown–rump length for later stages). **d**, Measurements of embryonic length at the indicated time points. Dots represent individual embryos; in utero, $n = 72, 25, 13, 19, 15, 38$ (left to right); ex utero, $n = 68, 29, 8, 19, 24$; **Mann–Whitney test; ns, not significant. **e**, Bright-field images of E5.5 embryos grown ex utero for 6 days until the 42-somite stage. Embryos cultured since E5.5 exhibit a mild developmental delay of about 2–4 pairs of somites when compared to those developed in utero; however, overall morphological development seemed to occur correctly. **f**, Percentages of normal embryos in cultures started at E5.5. **g**, Representative increase in size of embryos cultured from E5.5 to the hindlimb stage (6 days of culture). Embryos dissected at the beginning and end of culture are shown. **h**, Immunostaining of pre-gastrulating (E5.5) embryos cultured for 6 days until the 42-somite stage. LEFTY1 and OCT4 immunostaining on a section of an E5.5 embryo (left); GATA4, MHC-II and SOX2 maximum intensity projection of an embryo at culture day 6 and stained (right). Scale bars, 50 µm (E5.5 embryos), 500 µm (all others). *n*, total number of embryos; x, number of experiments; all data represent mean ± s.e.m. Images are representative of a minimum of three embryos.

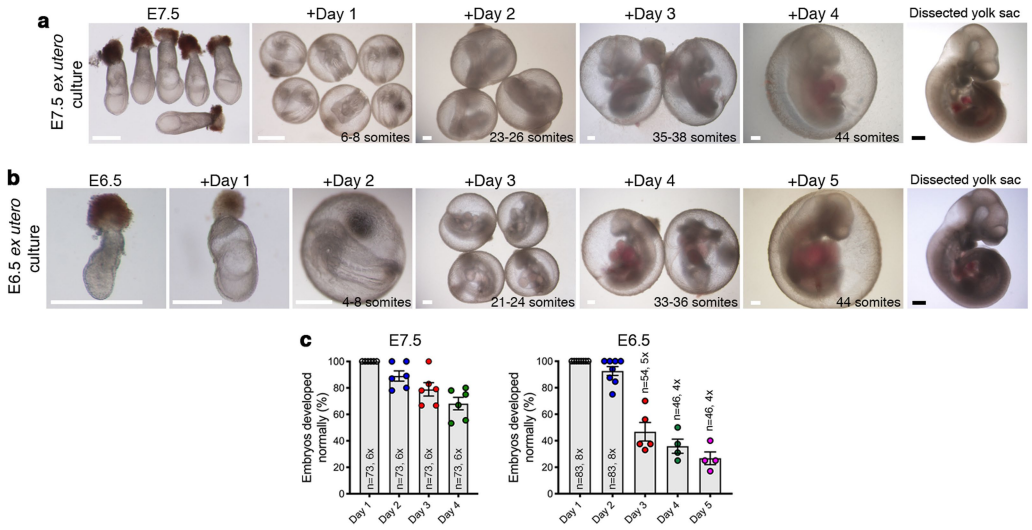

Extended Data Fig. 10 | Ex utero culture medium supplemented with HBS supports embryo development from early/late gastrulation until the hindlimb stage (E11). a, **b**, Bright-field microscopy images of mouse embryos grown ex utero from E7.5 (**a**) or E6.5 (**b**) with HCS replaced by in-house-prepared and freshly isolated adult HBS. **c**, Percentages of normal and defective embryos in cultures started at E7.5 and E6.5. *n*, total number of cultured embryos; x, number of experiments. Data represent mean ± s.e.m. Scale bars, 500 µm.

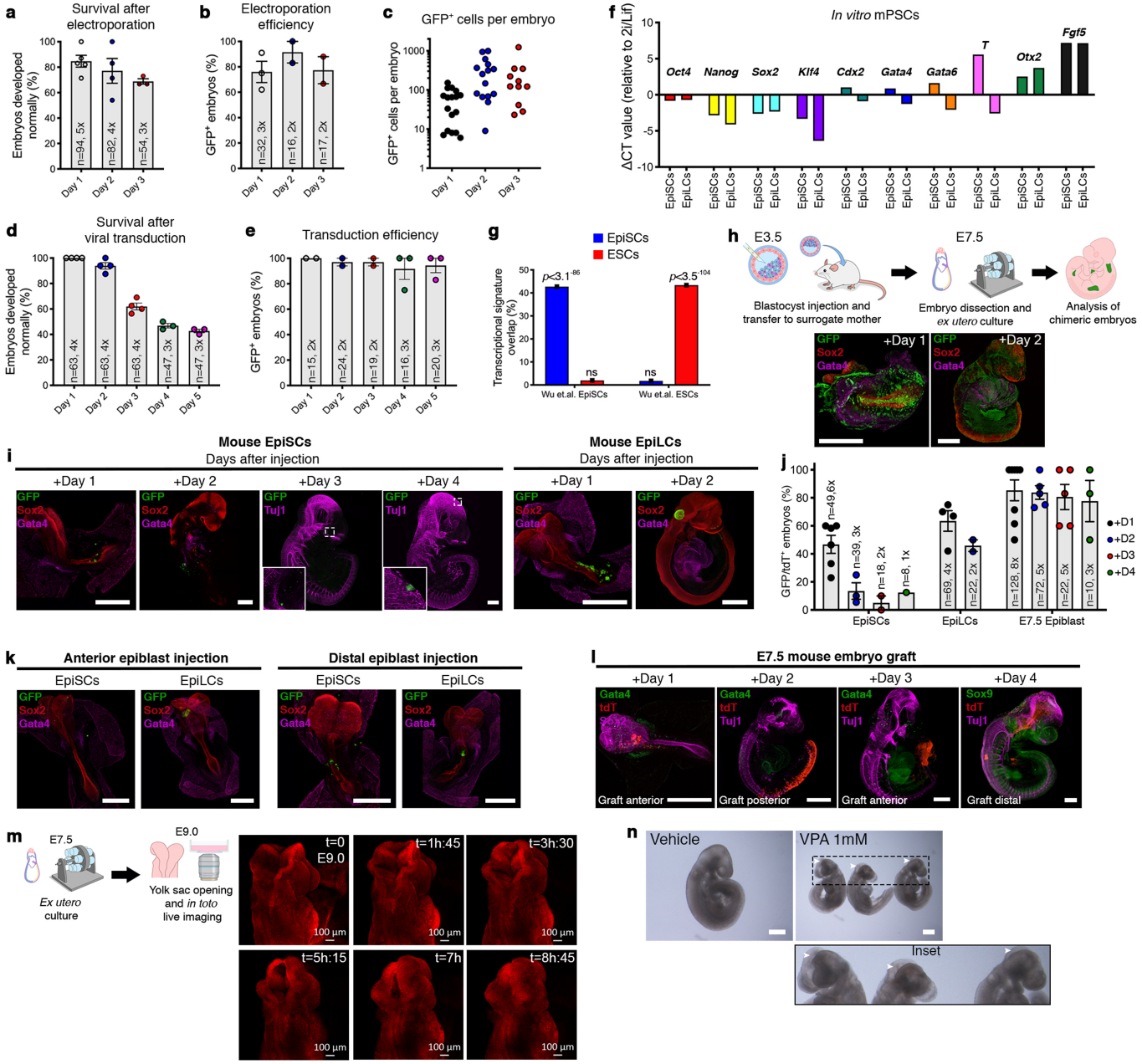

Extended Data Fig. 11 | Ex utero manipulation of mouse embryonic development. a, **b**, Percentages of developmentally normal (**a**) and GFP-expressing embryos (**b**) at 1–3 days after electroporation. **c**, Quantification of GFP$^+$ cells in electroporated embryos at the indicated times. Dots represent individual embryos. **d**, **e**, Percentages of normally developed (**d**) and GFP$^+$ embryos (**e**) after lentiviral transduction. Data represent mean ± s.e.m. **f**, Representative qPCR data showing the relative expression levels of mouse naive and primed markers in V6.5 mouse EpiS cells and formative EpiL cells, normalized to isogenic naive 2i/Lif ES cells. $n = 3$. **g**, Overlap in the transcriptional signature of differentially expressed genes measured by bulk RNA-seq in EpiS cells and ES cells used herein, compared to previously published datasets[26]. $n = 2$. **h**, Top, generation of mouse chimeras using isogenic naive ES cells. Bottom, GFP, SOX2 and GATA4 immunofluorescence images of chimeric embryos generated with naive ESCs. **i**, Whole-mount immunostaining of GFP$^+$ cells detected in embryos injected with mouse EpiS cells or EpiL cells at E7.5, cultured ex utero for 1–4 days and stained for GFP, SOX2 and GATA4. Insets are enlargements of the dashed boxes. $n \geq 8$ embryos. **j**, Percentages of chimeric embryos (GFP$^+$ or tdT$^+$) after micro-injection and ex utero culture. **k**, Immunostaining of +Day 1 cultured embryos injected with EpiS cells and EpiL cells in the anterior or distal epiblast. Images represent a minimum of three biological replicates. **l**, Representative confocal images of mouse post-implantation chimeras generated by tdT$^+$ E7.5 in vivo epiblast orthotopic transplantation followed by ex utero culture for 1–4 days, stained for tdTomato, GATA4 or SOX9 and SOX2 or TUJ1. $n \geq 10$ embryos. **m**, tdT$^+$ embryos explanted at E7.5 and subjected to in toto live imaging of neural tube closure at E9.0. $n = 3$. **n**, Embryos cultured ex utero since E7.5 and exposed to vehicle or 1 mM valproic acid (VPA) from E8.5 to E9.5. $n = 6$. Inset shows magnification of the dashed box. Arrowheads, neural tube closure defects. Scale bars, 100 µm (**m**), 500 µm (all others). *n*, total number of embryos assessed; x, number of experiments.

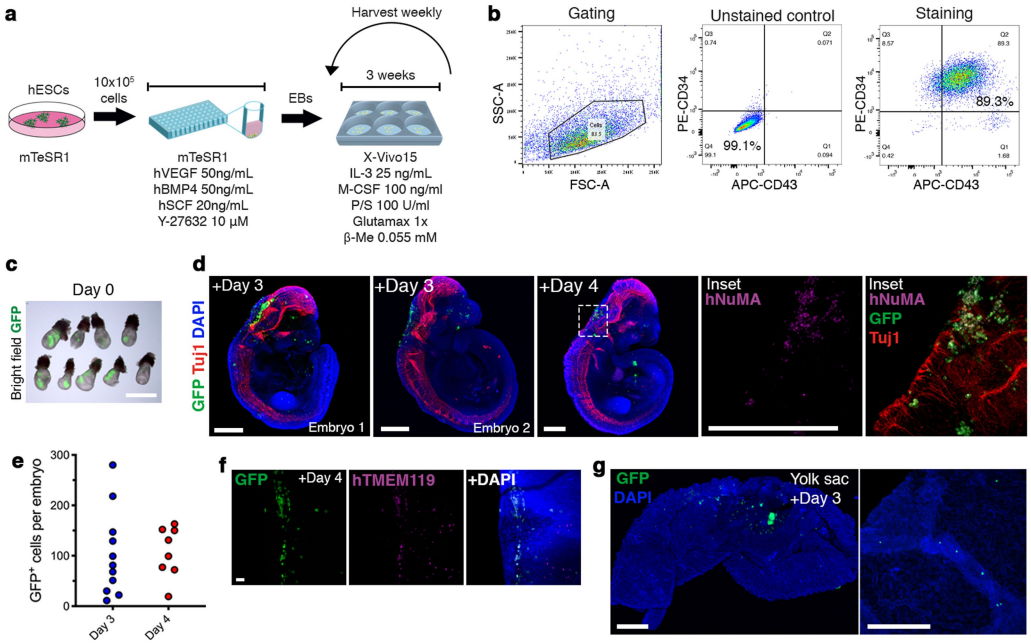

Extended Data Fig. 12 | Generation of human–mouse microglia interspecies chimeric embryos. a, Protocol for differentiation of microglia progenitors from humans ES cells as previously described[28]. **b**, Flow cytometry dot plot to validate the identity of obtained microglia cells by co-expression of the microglia progenitor cell markers CD34$^+$ and CD43$^+$. $n = 3$ independent experiments. **c**, Merged bright-field and fluorescence images of E7.5 embryos injected with GFP$^+$ human microglia progenitors at day 0. **d**, Representative immunofluorescence images of ex utero human microglia chimeric embryos 3 and 4 days after injection, labelled for GFP and TUJ1. The inset shows a magnification of the dashed box at day 4 identifying human nuclei (hNUMA), GFP and TUJ1. $n = 11$ embryos (day 3); $n = 8$ embryos (day 4). **e**, Quantification of GFP$^+$ cells detected in human–mouse microglia chimeric embryos (excluding GFP$^+$ cells found in the yolk sac). Dots represent individual embryos; $n = 11$ and 8 embryos for day 3 and day 4, respectively. **f**, Immunostaining for GFP and human TMEM119 in chimeric embryos. $n = 3$. **g**, Representative GFP immunofluorescence of a human microglia chimeric embryonic yolk sac and yolk sac vessel with circulating human GFP$^+$ cells. $n = 3$. Scale bars, 50 µm (**f**), 500 µm (all others).

nature research

Corresponding author(s): Jacob Hanna, Alejandro Aguilera, Itay Maza

Last updated by author(s): 17/02/21

Reporting Summary

Nature Research wishes to improve the reproducibility of the work that we publish. This form provides structure for consistency and transparency in reporting. For further information on Nature Research policies, see our Editorial Policies and the Editorial Policy Checklist.

Statistics

For all statistical analyses, confirm that the following items are present in the figure legend, table legend, main text, or Methods section.

n/a	Confirmed	
☐	☒	The exact sample size (*n*) for each experimental group/condition, given as a discrete number and unit of measurement
☐	☒	A statement on whether measurements were taken from distinct samples or whether the same sample was measured repeatedly
☐	☒	The statistical test(s) used AND whether they are one- or two-sided *Only common tests should be described solely by name; describe more complex techniques in the Methods section.*
☒	☐	A description of all covariates tested
☐	☒	A description of any assumptions or corrections, such as tests of normality and adjustment for multiple comparisons
☐	☒	A full description of the statistical parameters including central tendency (e.g. means) or other basic estimates (e.g. regression coefficient) AND variation (e.g. standard deviation) or associated estimates of uncertainty (e.g. confidence intervals)
☐	☒	For null hypothesis testing, the test statistic (e.g. *F*, *t*, *r*) with confidence intervals, effect sizes, degrees of freedom and *P* value noted *Give P values as exact values whenever suitable.*
☒	☐	For Bayesian analysis, information on the choice of priors and Markov chain Monte Carlo settings
☒	☐	For hierarchical and complex designs, identification of the appropriate level for tests and full reporting of outcomes
☒	☐	Estimates of effect sizes (e.g. Cohen's *d*, Pearson's *r*), indicating how they were calculated

Our web collection on statistics for biologists contains articles on many of the points above.

Software and code

Policy information about availability of computer code

Data collection	Single cell sequencing data were collected using Novaseq platform. Bulk RNA seq were collected with TrueSeq Illumina. qPCR data were obtained with the Viia7 platform (Applied Biosystems). Microscopy images were acquired with a Zeiss LSM 700 inverted confocal microscope (Carl Zeiss). 3D images of embryos were acquired with a light-sheet microscope (Ultramicroscope II, LaVision Biotec)
Data analysis	All statistical analysis besides single cell and bulk RNA-seq analysis were performed using the GraphPad Prism 8 software (La Joya, California). Fiji/Image J (version 1.52p) was used to count cell numbers. 10X Genomics data analysis was performed with the Cell Ranger 3.1.0 software (10x Genomics) and Seurat 3.0. The annotations were performed using the R package AUCELL 1.10.041, using parameters: aucMaxRank =100 (5% of the total gene count) under the AUCell_calcAUC function. To evaluate the probability of a certain cluster to be enriched to a certain tissue, we utilized the annotated AUC predictions of each cell to a tissue to compare to our observed cluster annotation of each cell, thus producing a p-value based on Mann-Whitney U statistics, this was performed using the R package roc.area v1.42 (CRAN.R-project.org). Differential expression (DEGs) of compatible clusters between in utero and ex utero was performed using parameters : fold-change-threshold of log(0.5) and with min.pct=0.25. DEGs with significant values were also enriched using the gene ontology database via R package limma 3.42.2 using function "goana". For bulk RNA seq, reads were trimmed with TrimGalore 0.6.5 (flags --stringency 3 --paired) and aligned to GRCm38 genome using STAR aligner (flags --runThreadN 64 --genomeLoad). Counts were estimated using HTSeq-count 0.7.2 (flags -q -f bam -r pos -s no -t exon -i gene_name). Normalization and differentially expressed genes were calculated using DESeq2 R package, with default parameters. External gene signatures, based on mouse microarray data, were calculated from GSE60603 (PMID 25945737). Flow cytometry was analyzed using FlowJo v10.7. Morphometric measurements were performed using the CellSens Entry 1.18 software (Olympus).

For manuscripts utilizing custom algorithms or software that are central to the research but not yet described in published literature, software must be made available to editors and reviewers. We strongly encourage code deposition in a community repository (e.g. GitHub). See the Nature Research guidelines for submitting code & software for further information.

Data

Policy information about availability of data

All manuscripts must include a data availability statement. This statement should provide the following information, where applicable:

- Accession codes, unique identifiers, or web links for publicly available datasets
- A list of figures that have associated raw data
- A description of any restrictions on data availability

The single cell RNA-seq and bulk RNA-seq data sets generated in this study have been deposited and publicly-available in the NCBI Gene Expression Omnibus (GEO; http://www.ncbi.nlm.nih.gov/geo) under accession number GSE149372. Source data are provided with this paper.

Field-specific reporting

Please select the one below that is the best fit for your research. If you are not sure, read the appropriate sections before making your selection.

☒ Life sciences ☐ Behavioural & social sciences ☐ Ecological, evolutionary & environmental sciences

For a reference copy of the document with all sections, see nature.com/documents/nr-reporting-summary-flat.pdf

Life sciences study design

All studies must disclose on these points even when the disclosure is negative.

Sample size	No statistical methods were used to predetermine sample size. The number of embryos used in each experiment was determined taking into account dat consistency, resources available and ethical reduction of animal use. For single cell RNA-Seq, the sample size was determined when the main cell lineages at each developmental stages were captured.
Data exclusions	For scRNA-seq, to filter out low expressing single cells, possible doublets produced during the 10X sample processing or single cells with extensive mitochondrial expression, we filtered out cells with under 200 expressing genes, over 4000 expressing genes or over 10% mitochondrial gene expression.
Replication	The exact number of replicate independent experiments and embryos is indicated in the figure or in the figure legend. All data refer to biological replicates. Single cell RNA-seq was performed in 2 biological replicates for E8.5/Day 2 and 5 &7 biological replicates for E10.5/+Day 4. All the attempts at replication were successful.
Randomization	Embryos were chosen randomly when placed in different culture conditions. Other experiments were not randomized.
Blinding	The investigators were not blinded to allocation during experiments and outcome assessment. We had no relevant scientific reasons to conduct blinding.

Reporting for specific materials, systems and methods

We require information from authors about some types of materials, experimental systems and methods used in many studies. Here, indicate whether each material, system or method listed is relevant to your study. If you are not sure if a list item applies to your research, read the appropriate section before selecting a response.

Materials & experimental systems

n/a	Involved in the study
☐	☒ Antibodies
☐	☒ Eukaryotic cell lines
☒	☐ Palaeontology and archaeology
☐	☒ Animals and other organisms
☐	☒ Human research participants
☒	☐ Clinical data
☒	☐ Dual use research of concern

Methods

n/a	Involved in the study
☒	☐ ChIP-seq
☐	☒ Flow cytometry
☒	☐ MRI-based neuroimaging

Antibodies

Antibodies used	Rabbit monoclonal anti-Brachyury (D2Z3J) (Cell Signaling Cat# 81694); Rabbit polyclonal anti-Cdx2 (Cell Signaling Cat# 3977); Mouse monoclonal anti-Cdx2 (Biogenex Cat# MU392A-UC); Goat polyclonal anti-Gata4 (Santa Cruz Cat# SC-1237); Rabbit polyclonal anti-Gata4 (Abcam Cat# Ab84593); Rabbit monoclonal anti-Foxa2 (Abcam Cat# Ab108422); Mouse monoclonal anti-Myosin Heavy Chain II (clone MF-20) (R&D Cat# MAB4470); Goat polyclonal anti-Otx2 (R&D Cat# AF1979); Rabbit polyclonal anti-Pax6 (Covance; Cat# PBR-278P); Goat polyclonal anti-Sox2 (R&D Cat# AF2018); Rabbit polyclonal anti-Sox9 (Millipore Cat# AB5535); Goat polyclonal anti-Sox17 (R&D Cat# AF1924); Mouse monoclonal anti-TUBB3 (Tuj1) (Covance Cat# MMS-435P); Chicken polyclonal anti-GFP (Abcam

Cat# Ab13970); Mouse monoclonal anti-Oct4 (clone C-10) (Santa Cruz Cat# SC-5279); Goat polyclonal anti-Lefty 1 (R&D Cat# AF746); Goat polyclonal anti-mCherry/Tomato (SiCGEN Cat# AB0040-200); Rabbit anti-hNUMA (Abcam Cat# ab84680); Rabbit polyclonal anti-human TEMEM119 (Invitrogen Cat# PA562505); Mouse monoclonal anti-human CD34-PE (BioLegend, Cat# 561), Mouse monoclonal anti-human CD43-APC (ebioscience, Cat# 84-3C1).

Validation

All the antibodies have been validated by the companies from which they were offered. Details of the validation statements, antibody profiles and relevant citations can be found on the manufacturer's website.
Antibodies for immunofluorescence: All antibodies were validated herein by immunofluorescence on mouse embryos, based on their well described expression patterns.
Rabbit monoclonal anti-Brachyury (Cell Signaling Cat# 81694). The antibody has been referenced in 5 publications: https://www.cellsignal.com/products/primary-antibodies/brachyury-d2z3j-rabbit-mab/81694
Rabbit polyclonal anti-Cdx2 (Cell Signaling Cat# 3977). The antibody has been referenced in 13 publications: https://www.cellsignal.com/products/primary-antibodies/cdx2-antibody/3977
Mouse monoclonal anti-Cdx2 (Biogenex Cat# MU392A-UC). The antibody has been referenced in more than 49 publications: https://store.biogenex.com/us/anti-cdx-2-clone-cdx2-130.html
Goat polyclonal anti-Gata4 (Santa Cruz Cat# SC-1237). The antibody has been referenced in 176 publications: https://www.scbt.com/p/gata-4-antibody-c-20
Rabbit polyclonal anti-Gata4 (Abcam Cat# Ab84593). The antibody has been referenced in 45 publications: https://www.abcam.com/gata4-antibody-ab84593.html
Rabbit monoclonal anti-Foxa2 (Abcam Cat# Ab108422). The antibody has been referenced in 42 publications: https://www.abcam.com/foxa2-antibody-epr4466-ab108422.html
Mouse monoclonal anti-Myosin Heavy Chain II (clone MF-20) (R&D Cat# MAB4470). The antibody has been referenced in 50 publications: https://www.rndsystems.com/products/myosin-heavy-chain-antibody-mf20_mab4470
Goat polyclonal anti-Otx2 (R&D Cat# AF1979). The antibody has been referenced in 37 publications: https://www.rndsystems.com/products/human-otx2-antibody_af1979
Rabbit polyclonal anti-Pax6 (Covance; Cat# PBR-278P). The antibody has been referenced in 169 publications: https://www.biolegend.com/en-us/products/purified-anti-pax-6-antibody-11511
Goat polyclonal anti-Sox2 (R&D Cat# AF2018). The antibody has been referenced in 93 publications: https://www.rndsystems.com/products/human-mouse-rat-sox2-antibody_af2018
Rabbit polyclonal anti-Sox9 (Millipore Cat# AB5535). Anti-Sox9 Antibody is a well characterized affinity purified Rabbit Polyclonal Antibody that reliably detects Transcription Factor Sox-9. This highly published antibody has been validated in IHC & WB: https://www.merckmillipore.com/INTL/en/product/Anti-Sox9-Antibody,MM_NF-AB5535?ReferrerURL=https%3A%2F%2Fwww.google.com%2F&bd=1
Goat polyclonal anti-Sox17 (R&D Cat# AF1924). The antibody has been referenced in 163 publications: https://www.rndsystems.com/products/human-sox17-antibody_af1924
Mouse anti-TUBB3 (Tuj1) (Covance Cat# MMS-435P). The antibody has been referenced in 436 publications. https://www.biolegend.com/en-us/products/purified-anti-tubulin-beta-3-tubb3-antibody-11580
Chicken polyclonal anti-GFP (Abcam Cat# Ab13970). The antibody has been referenced in 2036 publications: https://www.abcam.com/gfp-antibody-ab13970.html
Mouse monoclonal anti-Oct4 (clone C-10) (Santa Cruz Cat# SC-5279). The antibody has been referenced in 1905 publications: https://www.scbt.com/p/oct-3-4-antibody-c-10
Goat polyclonal anti-Lefty 1 (R&D Cat# AF746). Validated in for IHC in mouse tissues by a previous study. The antibody has been referenced in 1 publication: https://www.rndsystems.com/products/human-mouse-lefty-antibody_af746
Goat polyclonal anti-mCherry/Tomato (SiCGEN Cat# AB0040-200). This antibody (AB0040) recognizes very well tdTomato and does not recognize GFP (green fluorescent protein). The antibody has been referenced in 15 publications: https://www.origene.com/catalog/antibodies/primary-antibodies/ab0040-200/mcherry
Rabbit anti-hNUMA (Abcam Cat# ab84680). The antibody has been referenced in 6 publications: https://www.abcam.com/numa-antibody-ab84680.html
Rabbit polyclonal anti-human TEMEM119 (Invitrogen Cat# PA562505). This antibody has been validated by the manufacturer to react with human human cerebral cortex microglia. https://www.thermofisher.com/antibody/product/TMEM119-Antibody-Polyclonal/PA5-62505
Antibodies for immunohistochemistry:
Rabbit monoclonal anti-Foxa2 (Abcam Cat# Ab108422). Validated by the manufacturer using Formalin/PFA-fixed paraffin-embedded sections of mouse liver tissue. The antibody has been referenced in 42 publications: https://www.abcam.com/foxa2-antibody-epr4466-ab108422.html
Goat polyclonal anti-Gata4 (Santa Cruz Cat# SC-1237). Validated by the manufacturer for IHC in mouse tissues. The antibody has been referenced in 176 publications: https://www.scbt.com/p/gata-4-antibody-c-20
Antibodies for flow cytometry: All the antibodies guarantee covers the use of the antibody for flow cytometry applications.
Mouse monoclonal anti-human CD34-PE (BioLegend, Cat# 561). Each lot of this antibody is quality control tested by immunofluorescent staining with flow cytometric analysis. The antibody has been referenced in 8 publications: https://www.biolegend.com/en-us/products/pe-anti-human-cd34-antibody-6036
Mouse monoclonal anti-human CD43-APC (ebioscience, Cat# 84-3C1). This eBio84-3C1 (84-3C1) antibody has been pre-titrated and tested by flow cytometric analysis of human peripheral blood monocytes. The antibody has been referenced in 7 publications: https://www.thermofisher.com/antibody/product/CD43-Antibody-clone-eBio84-3C1-84-3C1-Monoclonal/17-0439-42

Eukaryotic cell lines

Policy information about cell lines

Cell line source(s)

Mouse V6.5 and WIS2 human embryonic stem cell lines were previously reported in Gafni et al. Nature 2013 and Geula et al. Science 2015. HEK293 was obtained from ATCC.

Authentication

Karyotype and sequencing data cofirmed expected sex, karyotype, gene reporters and SNPs.

Mycoplasma contamination	All cell lines tested negative for mycoplasma contamination by using the MycoAlert plasma Detection Kit (Lonza, Cat# LT07-318) and were routinely screened every 2 months.
Commonly misidentified lines (See ICLAC register)	None were used herein

Animals and other organisms

Policy information about studies involving animals; ARRIVE guidelines recommended for reporting animal research

Laboratory animals	All mice were housed in a standard 12-hour light/12-hour dark cycle conditions in a specialized and certified animal facility. 5-8 weeks old female mice (mus musculus) of the strains ICR, C57BL/6, 129 and BDF1 were mated with male (5-40 weeks old) ICR, BDF1 or C57/B6 mice. Established transgenic mouse strains used were: Jackson #007576, Jackson #022137, Jackson #024242, Jackson #007914, Jackson #030539
Wild animals	The study did not involve wild animals
Field-collected samples	The study did not involve samples collected from the field
Ethics oversight	All animal experiments were performed according to the Animal Protection Guidelines of Weizmann Institute of Science, Rehovot, Israel. All animal experiments described herein were approved by relevant Weizmann Institute IACUC (#01390120-1, 01330120-2, 33520117-2).

Note that full information on the approval of the study protocol must also be provided in the manuscript.

Human research participants

Policy information about studies involving human research participants

Population characteristics	Healthy pregnant women who were asked to give their informed consent to have blood collected from their umbilical cord, as approved by a Rambam Medical Center Helsinki committee (#RMB-0452-15). The source of each collection underwent full anonymization and was not identified by name or other designation, and the extracted serum was only used as described herein. Healthy women over the age of 18 and under 40, who gave their consent and were scheduled for caesarian section delivery by their obstetrician following a prenatal clinic visit, were eligible for cord blood collection. We excluded women who gave vaginal birth as well as women with any chronic illness or active medical conditions, including gestational diabetes or hypertension. All adult blood samples were collected from healthy donors.
Recruitment	Research donors in the study were recruited from the prenatal clinic at the Rambam Medical Center were asked to give their informed consent to have blood collected from their umbilical cord. Adult blood samples were collected from the authors of the study.
Ethics oversight	Rambam Medical Center Helsinki committee (#RMB-0452-15)

Note that full information on the approval of the study protocol must also be provided in the manuscript.

Flow Cytometry

Plots

Confirm that:

☒ The axis labels state the marker and fluorochrome used (e.g. CD4-FITC).

☒ The axis scales are clearly visible. Include numbers along axes only for bottom left plot of group (a 'group' is an analysis of identical markers).

☒ All plots are contour plots with outliers or pseudocolor plots.

☒ A numerical value for number of cells or percentage (with statistics) is provided.

Methodology

Sample preparation	Cells were incubated for half an hour with CD34-PE (BioLegend, 561) and CD43-APC (ebioscience, 84-3C1) antibodies (1:50) on PBS/0.5% BSA.
Instrument	BD FACS-Aria III
Software	FlowJo v10.7
Cell population abundance	Only one cell population was analyzed and the purity was verified
Gating strategy	FSC and SSC singlets were gated to remove debris and aggregated cells, and only single cells were considering for all analyses. To determine the gating for positive of negative populations, an unstained control was employed, making sure that 100% of the unstained population was allocated on the negative area of the histogram/dot plot. Gating strategies are shown in

Extended Data Fig. 12b.

☒ Tick this box to confirm that a figure exemplifying the gating strategy is provided in the Supplementary Information.